

NEURAL MECHANISMS IN PROCESSING OF EMOTION IN REAL AND
VIRTUAL FACES USING FUNCTIONAL-NEAR INFRARED SPECTROSCOPY
(FNIRS)

by

Dylan Rapanan

A thesis submitted to the
School of Graduate and Postdoctoral Studies
in partial fulfillment of the requirements for the degree of

Masters of Science in Computer Science

Faculty of Science
Ontario Tech University
Oshawa, Ontario, Canada

© Dylan Rapanan 2025

Abstract

As avatars permeate social media, gaming, and telecommunications, understanding how the brain reads emotions from virtual faces is increasingly important. We recorded functional near-infrared spectroscopy (fNIRS) data from adults viewing real photographs and matched computer-generated faces expressing Anger, Disgust, Fear, Joy, Sadness, Surprise, or Neutrality. General-linear-model mapping revealed differences in activation between multiple brain regions. Functional-connectivity analysis provided insights into synchronization between brain regions in the time-frequency domain, finding differences in synchrony across certain brain regions. Collectively, the results demonstrate differences primarily in the visual cortex across face and emotion types, and across other brain regions, including the left prefrontal and right parietal regions. These neural signatures provide quantitative targets for refining the realism and emotional efficacy of digital characters in virtual and augmented environments.

Acknowledgements

** Put your Acknowledgements here. ***

Contents

Abstract	ii
Acknowledgment	iii
1 Introduction	1
2 Methodology	2
2.1 Participants	2
2.2 Stimuli	3
2.3 Design and Procedure	4
2.3.1 Procedure	4
2.4 fNIRS data	6
2.5 Analysis	8
2.5.1 Preprocessing Steps	9
2.5.2 Epochs	10
2.5.3 General Linear Model (GLM) Analysis	10
Design Matrix	11
Contrast Computation	12
2.5.4 Functional Connectivity Analysis	12
Paired Sample t-tests	14
ROI Chord Plots	15

2.5.5	Memory Task Analysis	15
3	Results	18
3.1	General Linear Model (GLM) Results	18
3.1.1	Face Type Contrasts	18
3.1.2	Emotion Contrasts	19
3.1.3	Face Type \times Emotion Contrasts	22
3.2	Functional Connectivity Results	23
3.2.1	Face Type Contrasts	23
3.2.2	Emotion Contrasts	24
3.2.3	Face Type \times Emotion Contrasts	28
3.3	Memory Task Results	29
4	Discussion	31
4.1	Limitations and Future Directions	31
4.2	Conclusion	31
Bibliography		31
Appendix		36
A	GLM Contrasts	37
B	Functional Connectivity Contrasts	42
C	Memory Task ANOVA Table	49

List of Tables

A.1	Table of contrast results from the GLM analysis.	37
B.1	Group level <i>t</i> -tests and Sum of Significantly different channels averaged across ROIs.	43
C.1	Two-way ANOVA results for the effect of Face Type and Emotion and their interaction on the correct responses.	49

List of Figures

2.1	SCI signal quality inclusion threshold	3
2.2	Experimental paradigm overview	6
2.3	Montage depictions	7
2.4	Brain region map for ROI grouping	8
2.5	Preprocessing steps for fNIRS data	9
2.6	Sample design matrix for GLM	12
2.7	Chord plot for Sadness condition	14
2.8	Correct responses by participant	16
3.1	GLM: Real vs. Virtual Faces	18
3.2	GLM: Emotion vs. Neutral	19
3.3	GLM: Emotion vs. Surprise	20
3.4	GLM: Neutral vs. Surprise	21
3.5	GLM: Face Type \times Emotion Contrasts	22
3.6	FC: Real vs. Virtual	23
3.7	FC: Emotion Contrasts (Fear and Anger)	24
3.8	FC: Summary of Contrasts by Emotion Pair	25
3.9	FC: Count of Significantly Different Channel Pairs by ROI	26
3.10	FC: Face Type \times Emotion Contrasts	28
3.11	Correct Memory Task Responses by Face Type and Emotion	29

B.1 FC: Additional emotion contrasts	42
--	----

Chapter 1

Introduction

Chapter 2

Methodology

2.1 Participants

Participants were recruited from Ontario Tech University’s SONA system. In total, 91 participants completed the study, however 4 were removed due to recording/presentation issues. Signal quality was assessed by computing the Peak Spectral Power (PSP) and the Scalp Coupling Index (SCI) ([Pollonini et al., 2016](#)) over sliding windows (5 seconds in duration) across all channels, similar to the methods used by ([Bulgarelli et al., 2025](#)) and ([Hernandez and Pollonini, 2020](#)). Sliding windows of 5 seconds were taken from each channel, and Peak Spectral Power (PSP) and the Scalp Coupling Index (SCI) were calculated for each window. Participants were included in the analysis if they met the following quality assurance criteria: 1) PSP > 0.1 and SCI > 0.5 (based on ([Holmes et al., 2024](#))) for more than 70% of the windows in a single channel, the channel was considered to have good signal quality, and 2) > 70% of the channels for a single participant were considered to have good signal quality, the participant was included in the analysis. There were 35 data that did not meet the quality assurance criteria and were excluded from subsequent analyses. A total 52 participants (Figure [2.1](#)) were included in the final analyses. The 52 participants ranged in age from 17 to 51 (M = 21.65, SD = 6.71), 39/52

were female, and no demographic information was collected. The study was approved by Ontario Tech’s Research Ethics Board (REB).

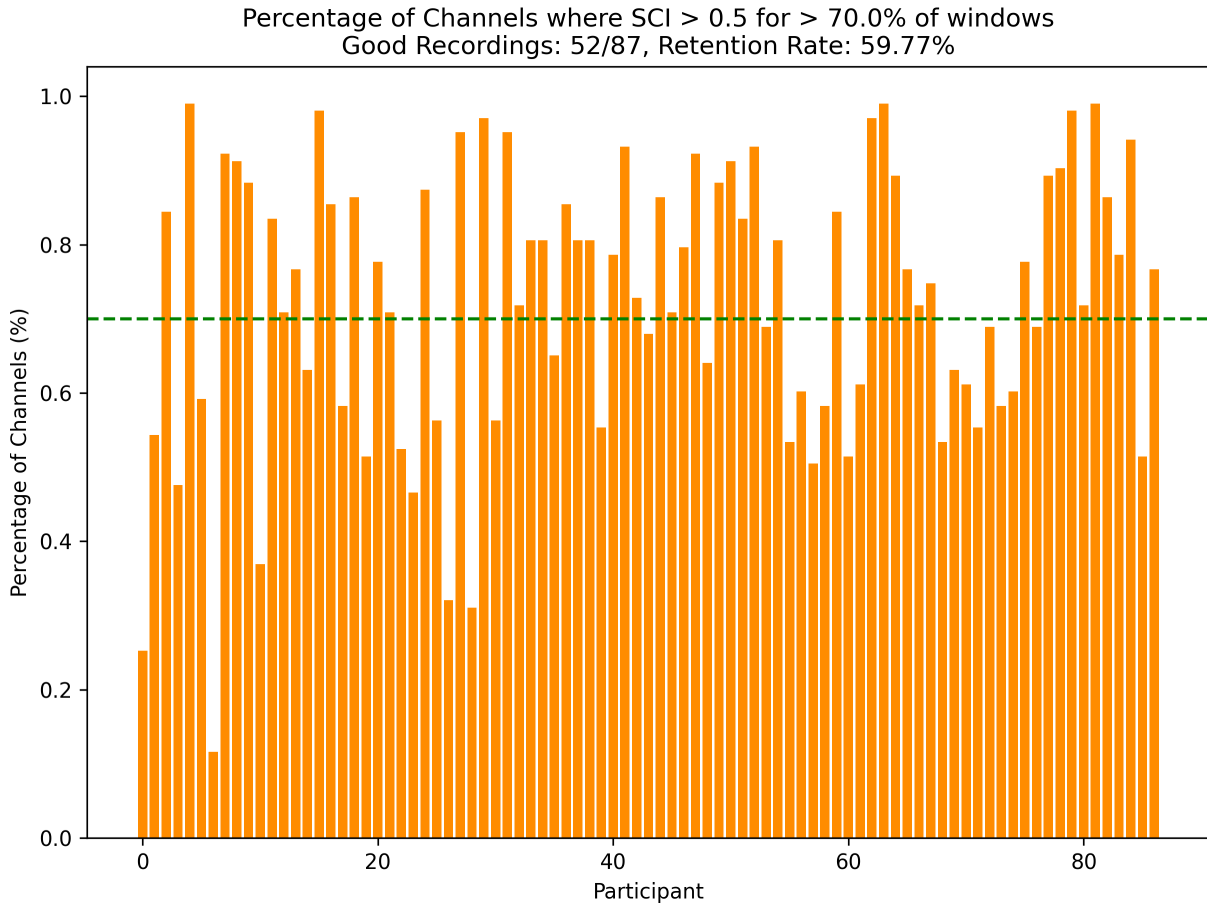


Figure 2.1: Percentage of Channels where SCI > 0.5 for $> 70\%$ of the windows. The green dashed line represents the threshold of 70% of windows that each participant must meet to be included in the analysis.

2.2 Stimuli

Face stimuli were selected from two large publicly available repositories: the RADIATE dataset ([Conley et al., 2018](#)) and the UIBVFED dataset ([Oliver and Amengual Alcover, 2020](#)). The RADIATE dataset contains 109 images of racially and ethnically diverse real people, aged 18-30 years old expressing 16 emotions. The UIBVFED dataset contains a set of 20 virtual characters that are also ethnically diverse, aged 20-80 years old expressing

32 emotions. The UIBVFED faces were created ([Oliver and Amengual Alcover, 2020](#)) using blendshapes, a tool that represents and manipulates facial action units ([Ekman and Friesen, 1978](#)). The faces used in the current study were based on the following criteria: 1) 20 young adult models were selected, 5 males, 5 females from both datasets (RADIATE and UIBVFED), 2) The corresponding models from each dataset were matched for face shape, sex, skin tone, and hair color, and 3) 7 emotional expressions (anger, disgust, fear, happiness, sadness, surprise, neutral) were selected for each model, that closely align with Ekman's 6 basic emotions + neutral ([Ekman, 1992](#)). The UIBVFED images were cropped to the same size as the RADIATE images, for consistency in the stimuli presentation. The stimuli presentation was prepared using PsychoPy3 Experiment Builder (v2024.1.5) ([Peirce et al., 2019](#)).

2.3 Design and Procedure

2.3.1 Procedure

The stimuli were presented on a Dell U2415 24 inch 1920x1200 60Hz monitor, placed at eye level, and the participants were seated in a comfortable chair facing the monitor. The beginning of the stimuli presentation had instructions on the screen, which explained the task to the participant, and the participant entered the space bar when they were ready to start the experiment. We used a repeated-measures design consisting of four within-subjects factors: 1) Face Type (Real, Virtual), 2) Emotion (Anger, Disgust, Fear, Joy, Sadness, Surprise, Neutral), 3) Model (10 unique identities per face type), and Sex (Male, Female). Each participant saw 28 repetitions of each Face Type, 8 repetitions of each emotion across 56 blocks, each comprising eight faces (4 male, 4 female) of the same face type and emotional expression, counterbalanced across Face Type and Emotion. Between every block and starting the experiment, there is a fixation cross presented for 16 seconds. The 8 faces (4 male, 4 female, randomly selected) are presented one at a time, for 1.5

seconds each, with a 250-750 ms (mean 500 ms) interstimulus interval (ISI) between each face. To ensure participants remained engaged and focused on the emotions and faces, they also completed a memory task at the end of each block. That is, participants saw blocks of 8 faces, and after each block, there will be a 9th face, and they will need to indicate whether the 9th face was in the previous block of 8 faces. The participant was instructed to press 'y' on the keyboard if the face was in the previous block, or 'n' if the face was not in the previous block. The 9th face has a 50% chance of either being in the previous block or not, and if the participant does not respond within 7 seconds, the presentation will continue to the next block. Every 7 blocks, the participants are given a break, and prompted to enter the space bar when they are ready to continue the experiment. This task is visualized in Figure 2.2.

Brain activity was recorded using Aurora fNIRS while participants completed the task. Head size was measured and an fNIRS cap was fitted to their head. A signal optimization routine (in Aurora fNIRS) then increases the source brightness in a stepwise manner, until the optimal signal levels for all channels is reached. The signal level is the voltage reading at a detector optode, which reflects how well light passes through the tissue from a source optode to a detector optode. Participants were told that a series of faces each expressing different emotions would appear one at at time on the screen, and at the end of each block they would be asked whether a probe face matched one of the faces they saw in during the block they just completed. The experimenter(s) then turned the lights off in the room to avoid any interference with the fNIRS cap. Then the experimenter(s) started the experiment, and left the room to minimize noise and distractions. Experimenter(s) then monitored the experiment from outside the room, using a camera in the testing room. After the experiment was completed (approximately 35 minutes), the experimenter(s) entered the room, removed the fNIRS cap, and the participant was debriefed about the experiment.

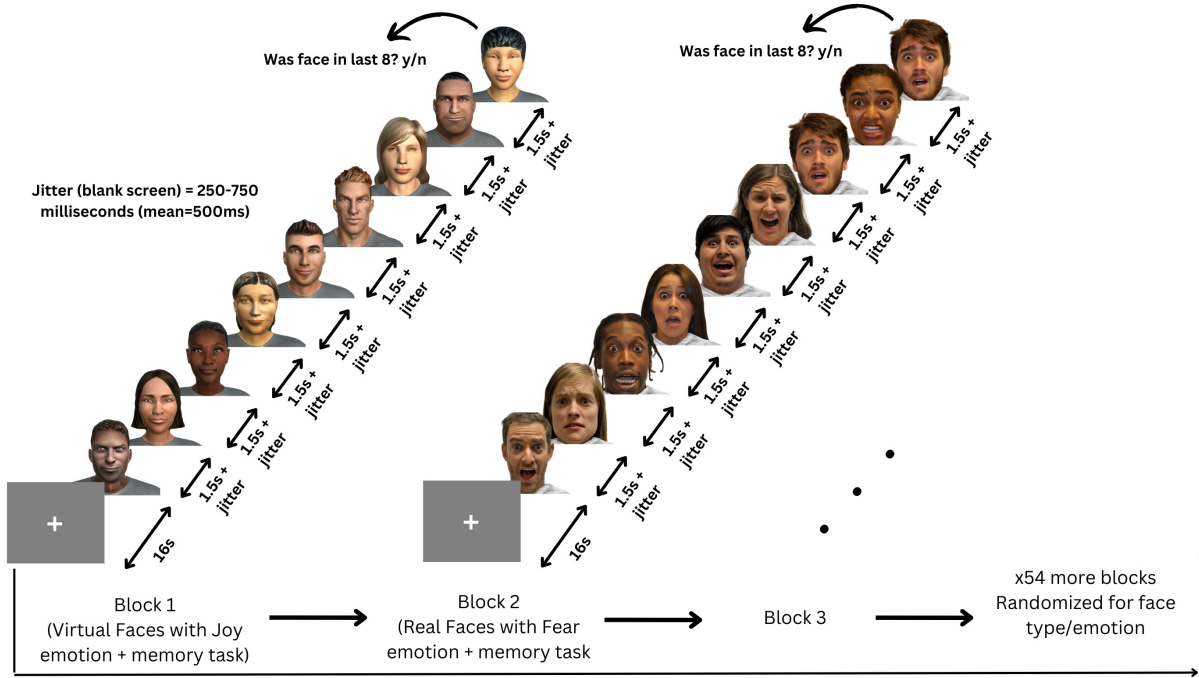
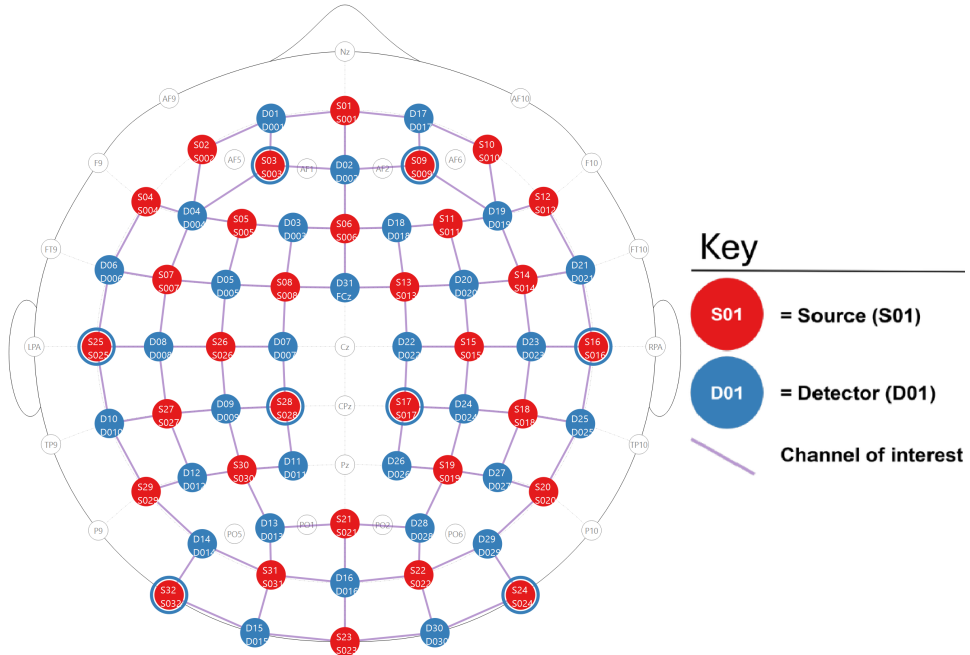


Figure 2.2: Participants viewed 56 blocks of 8 faces, each block being either all real or all virtual faces. Every face in a block displayed the same emotional expression, one of: anger, disgust, fear, happiness, sadness, surprise, neutral.

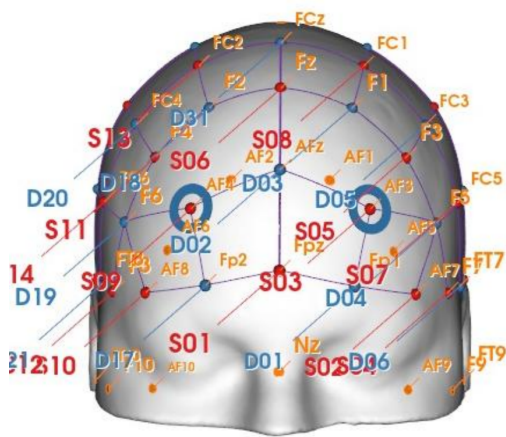
2.4 fNIRS data

fNIRS data was collected using two NIRSport2 systems (NIRx Medical Technologies, Berlin, Germany). Each NIRSport2 system was equipped with 16 source and 16 detector optodes, and daisy-chained together for a high density 32x32 optode configuration. Each neighboring pair of source and detector optode is referred to as a channel, resulting in a total of 103 HbO + 103 HbR channels (plus 16 short distance channels). The average distance between source and detector optodes was 30 mm, and 7mm for short distance channels, which were placed on a flexible fNIRS head cap (NIRScap) 58 cm in circumference. The optodes were arranged in a high density 32x32 montage with one bundle of short distance channels, as shown in Figure 2.3. This montage was designed to cover a maximally large area of the brain, given increasing evidence that emotion processing is not localized to specific discrete areas of the brain, rather distributed across

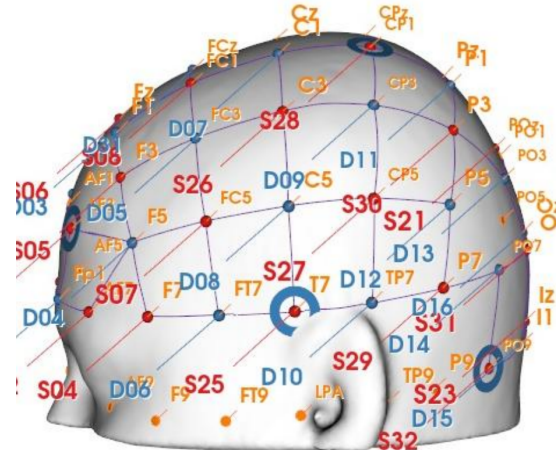
the brain (Lindquist et al., 2012). The fNIRS cap and optodes were positioned following the 10-20 international coordinate system. Light was emitted at 760 nm and 850 nm wavelengths, and the sampling rate was approximately 6.105 Hz.



(a) 2D depiction of the montage.



(b) 3D front view of the montage.



(c) 3D side view of the montage.

Figure 2.3: Depictions of the high density 32x32 optode montage. Red circles represent sources, blue circles represent detectors, purple lines represent channels, and blue rings around sources represent the locations of the 8 short distance detectors.

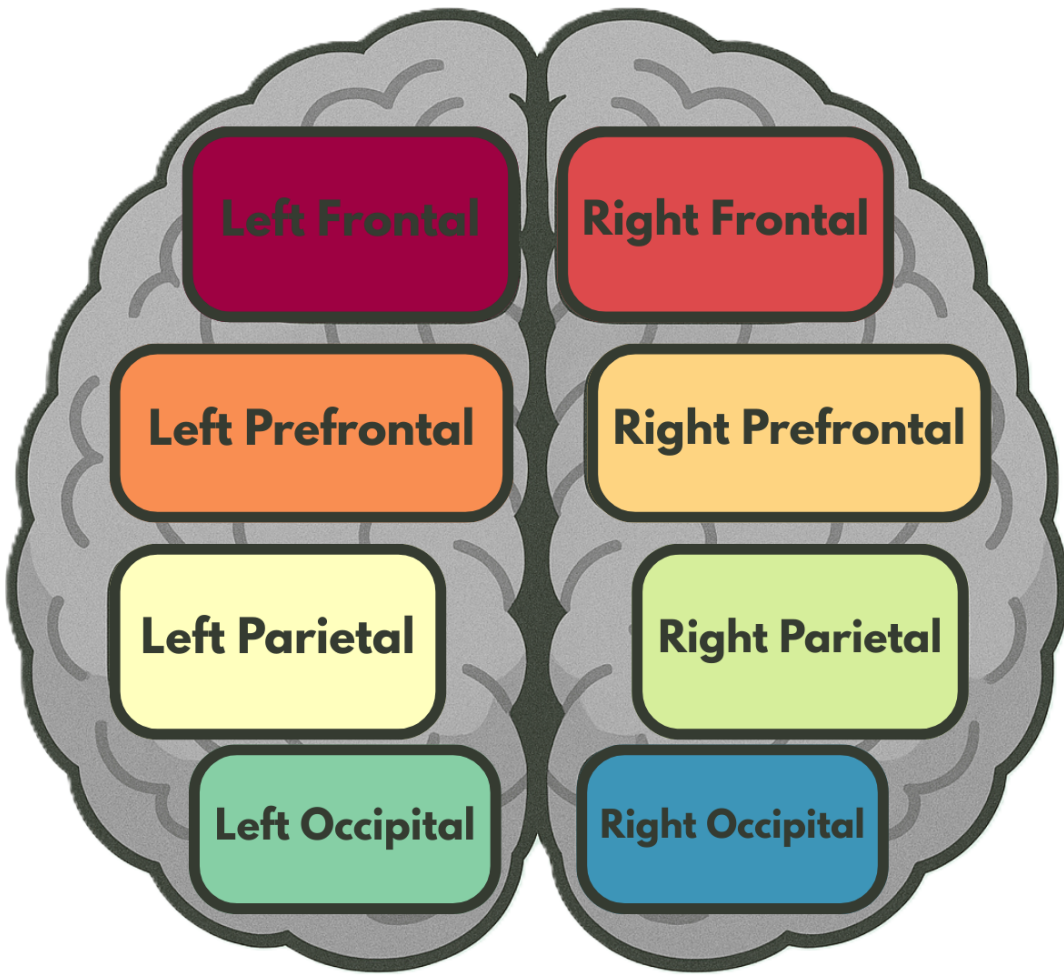


Figure 2.4: Brain region map, showing the regions of interest (ROI's) that the channels were grouped into for certain analyses.

2.5 Analysis

All fNIRS data was preprocessed and analyzed with Python 3.11.9 using MNE (version 1.9.0) ([Gramfort et al., 2013](#)) and MNE-NIRS (version 0.7.1) ([Luke et al., 2021](#)), which used the Nilearn package (version 0.9.2). First, the General Linear Model (GLM) analysis was performed, followed by a functional connectivity analysis performed on the same set of data. The memory task was analyzed on the y/n responses discussed in [2.3.1](#).

2.5.1 Preprocessing Steps

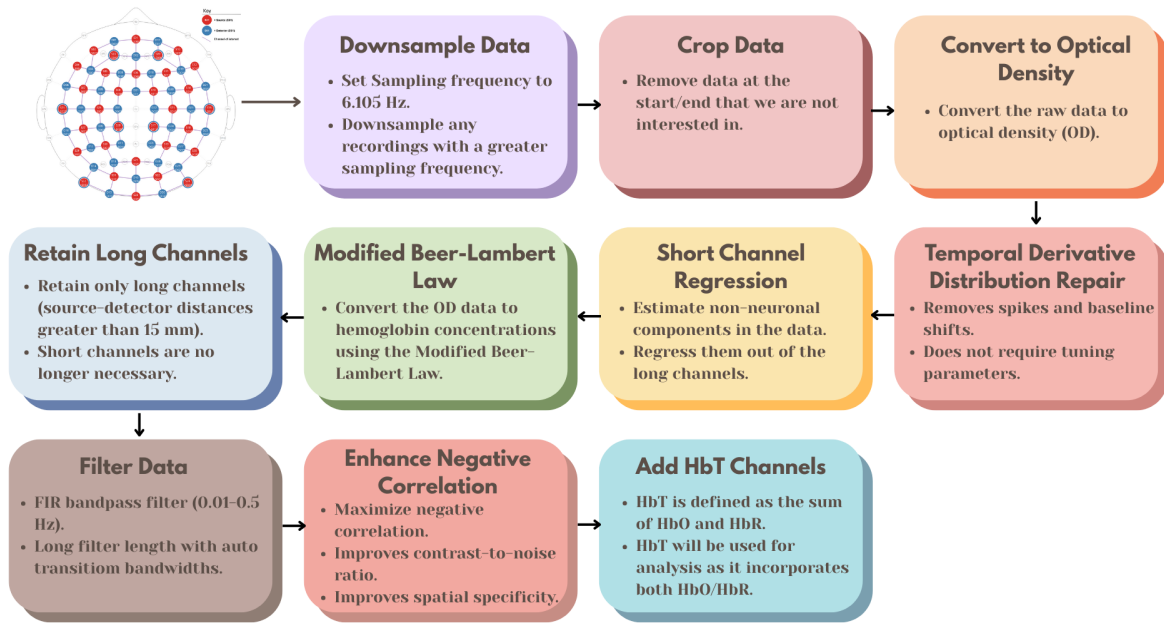


Figure 2.5: Preprocessing steps for fNIRS data, from the raw data to the fully processed data.

The preprocessing steps for the fNIRS data, as shown in Figure 2.5, were as follows:

- 1) Downsample the data if the sampling frequency is greater than 6.105 Hz, the initial two datasets were sampled higher than 6.105 Hz, and the sampling frequency should be consistent across all datasets.
- 2) Crop the data to the first and last annotation. This gets rid of the extra data at the beginning and end of the recording that are not of interest.
- 3) Convert the raw data to optical density.
- 4) Apply temporal derivative distribution repair to the OD data (Fishburn et al., 2019). TDDR is effective at removing spikes and baseline shifts from the data.
- 5) Apply short channel regression to the OD data (Scholkmann et al., 2014). Short channels are used to estimate the superficial hemodynamics (non-evoked/extracerebral/systemic components) in the data, and then regress it out of the long channels (Tachtsidis and Scholkmann, 2016).
- 6) Convert the OD data to hemoglobin concentrations using the modified Beer-Lambert law. The MBLL relates the change in light attenuation to the change in hemoglobin concentration of chromophores in the

tissue (Kocsis et al., 2006). 7) Retain only long channels (source-detector distance > 15 mm). Since the short channels have already been regressed out, it is no longer necessary to keep them in the data. 8) This FIR bandpass filter extracts signal components in the 0.01-0.5 Hz range, it uses a long filter length (2015 samples) with automatically determined transition bandwidths by MNE-Python (Pinti et al., 2019). 9) Maximizes negative correlation between HbO and HbR (Cui et al., 2010). This method removes spikes, improves contrast-to-noise ratio, and improves spatial specificity of the data. 10) Add HbT (hemoglobin total) channels to the data. HbT is defined as the sum of HbO and HbR. Often, fNIRS studies will only use either one of HbO or HbR channels (more frequently HbO), leaving out one channel with no justification (Kinder et al., 2022). Therefore, HbT channels are chosen, as HbT makes use of both HbO and HbR channels, and using both hemoglobin species improves the inferences as to where activation occurs (Hocke et al. (2018)).

2.5.2 Epochs

Variable length epochs were created for each block of 8 faces, which were 14-18 seconds long (mean = 16s), depending on the ISI's (see 2.3.1). Epochs were sorted by Face Type (Real, Virtual), and Emotion (Anger, Disgust, Fear, Happiness, Sadness, Surprise, Neutral). Baseline correction was applied to remove any constant or slowly varying offsets in the data. The data was annotated with the onsets and offsets of each block, along with the duration and condition of each block for use in section 2.5.3 and 2.5.4.

2.5.3 General Linear Model (GLM) Analysis

The General Linear Model (GLM) posits that the observed haemodynamic signal at each channel or Region of Interest (ROI) is a linear combination of task-related regressors convolved with a Hemodynamic Response Function (HRF), plus nuisance regressors (e.g., drift) and residual noise. Mathematically,

$$Y = X\beta + \epsilon, \quad (2.1)$$

where Y is the observed time series, X is the design matrix, β represents the parameters to estimate, and ϵ denotes the residuals assumed to be (i.i.d.) Gaussian noise. Estimation is performed via ordinary least squares (OLS), yielding parameter estimates that quantify condition-specific activation amplitudes.

Design Matrix

For each of the epochs, events are defined by their trial type (e.g., emotion or face type), and onsets/offsets relative to the procedure start, and duration. The design matrix is constructed using Nilearn's `make_first_level_design_matrix` by convolving a boxcar function (based on the event timing) with a canonical HRF, which is a model of the expected haemodynamic response to neural activity. The canonical HRF Statistical Parametric Mapping (SPM) ([Friston, 2007](#)) is chosen to model neurovascular coupling, this model captures the stereotypical rise and fall of the BOLD/fNIRS response. The cosine drift model was utilized, which incorporates discrete cosine transform (DCT) basis functions into the design matrix to model and remove low-frequency drifts. The selection of the high pass cutoff frequency is guided by the structure of the experimental design. The cutoff period is set to twice the duration of the longest inter-trial interval, and each fixation period between epochs (or blocks) is 16 seconds. Therefore, a cutoff period of 32 seconds (i.e., `high_pass=0.03125 Hz`) would be appropriate. This ensures that the drift model does not remove task-related signal components that occur at frequencies higher than the cutoff ([Luke et al., 2021](#)). The design matrix X and preprocessed time series are fed into MNE's `run_glm` function, which computes OLS estimates of β for each channel.

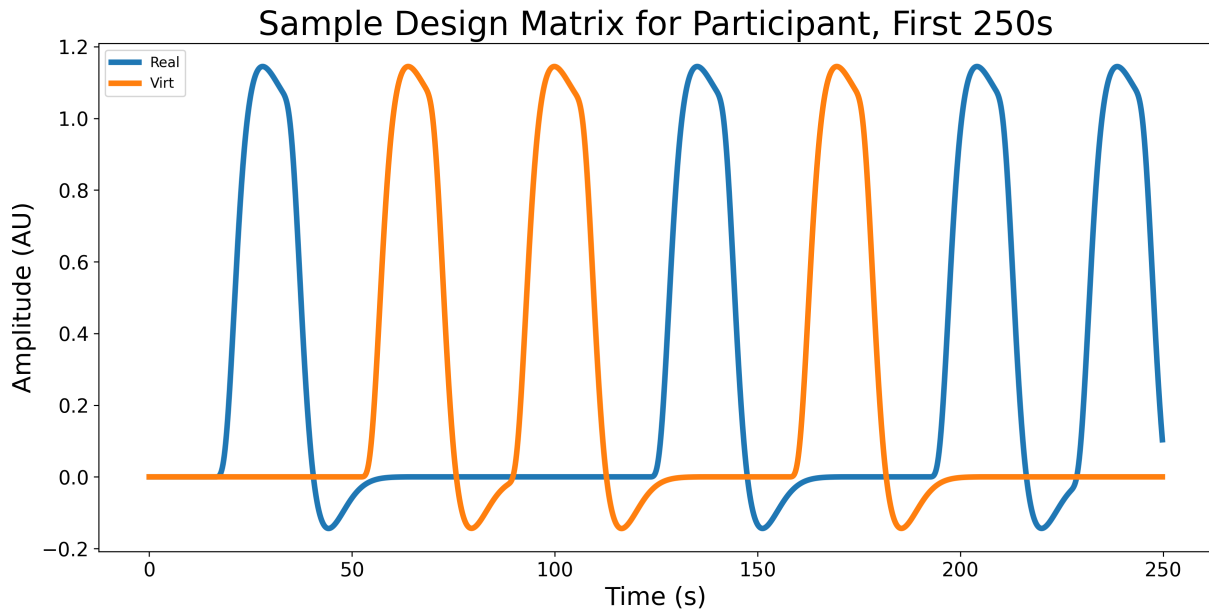


Figure 2.6: Sample design matrix for a single participant for the effect Face type, showing the first 7 blocks (250 seconds) of a single experiment. The design matrix is organized by condition (Blue for real, orange for virtual), this is the result of convolving the boxcar function with the canonical HRF SPM.

Contrast Computation

All pairwise contrasts were generated between conditions by constructing an identity contrast matrix over design columns. For each pair of conditions (A, B), the contrast vector is defined as: $c = e_A - e_B$, where e_A and e_B are the respective design matrix columns for conditions A and B . Contrasts are computed using MNE's `compute_contrast` function, which produces effect estimates and test statistics aggregated across channels. Since numerous statistical tests are performed across channels and contrasts, p -values were corrected for false discovery rate (FDR) using the Benjamini-Hochberg procedure ([Singh and Dan, 2006](#)) with a family-wise error rate of $\alpha=0.05$.

2.5.4 Functional Connectivity Analysis

To characterize the temporal coordination between fNIRS channels during face and emotion processing, functional connectivity matrices were computed using a continuous

wavelet transform (CWT)-based spectral connectivity approach. CWT decomposes signals into simultaneous time-frequency representations, providing an optimal framework for fNIRS connectivity analysis by accommodating the non-stationary, physiological nature of hemodynamic signals. The morlet wavelet, a gaussian function modulated by a sine wave, was picked as they are suited to capture both slow neural rhythms and faster systemic fluctuations in fNIRS data (Reddy et al., 2021). Wavelet-based approaches have been widely adopted in the fNIRS literature for connectivity and even artifact correction (Bergmann et al., 2023; Hakim et al., 2023) Coherence combines both phase and amplitude information into a single, normalized index, 0 (no coupling) to 1 (perfect coupling), and is a richer description of coupling than phase-only or amplitude-only metrics (Bastos and Schoffelen, 2016). For each participant, MNE’s `spectral_connectivity_time` function was applied to compute time-resolved coherence across pairs of channels, the average of this was taken across epochs to obtain a single channel-by-channel connectivity matrix for each condition. Each participants’ connectivity matrix was then averaged across participants to obtain a group-level connectivity matrix for each condition, an example of a group-level connectivity chord plot is shown in Figure 2.7. fNIRS hemodynamics predominantly fluctuate in very low frequencies (0.01-0.5 Hz) (Reddy et al., 2021). The frequency range was narrowed to five evenly spaced frequencies between 0.2-0.5 Hz due to short epoch length, this range still targets systemic and neurogenic oscillations while avoiding high-frequency noise (Xu et al., 2017). Averaging across these closely spaced frequencies reduces data dimensionality, simplifying downstream statistical analyses without sacrificing sensitivity to coupling dynamics.

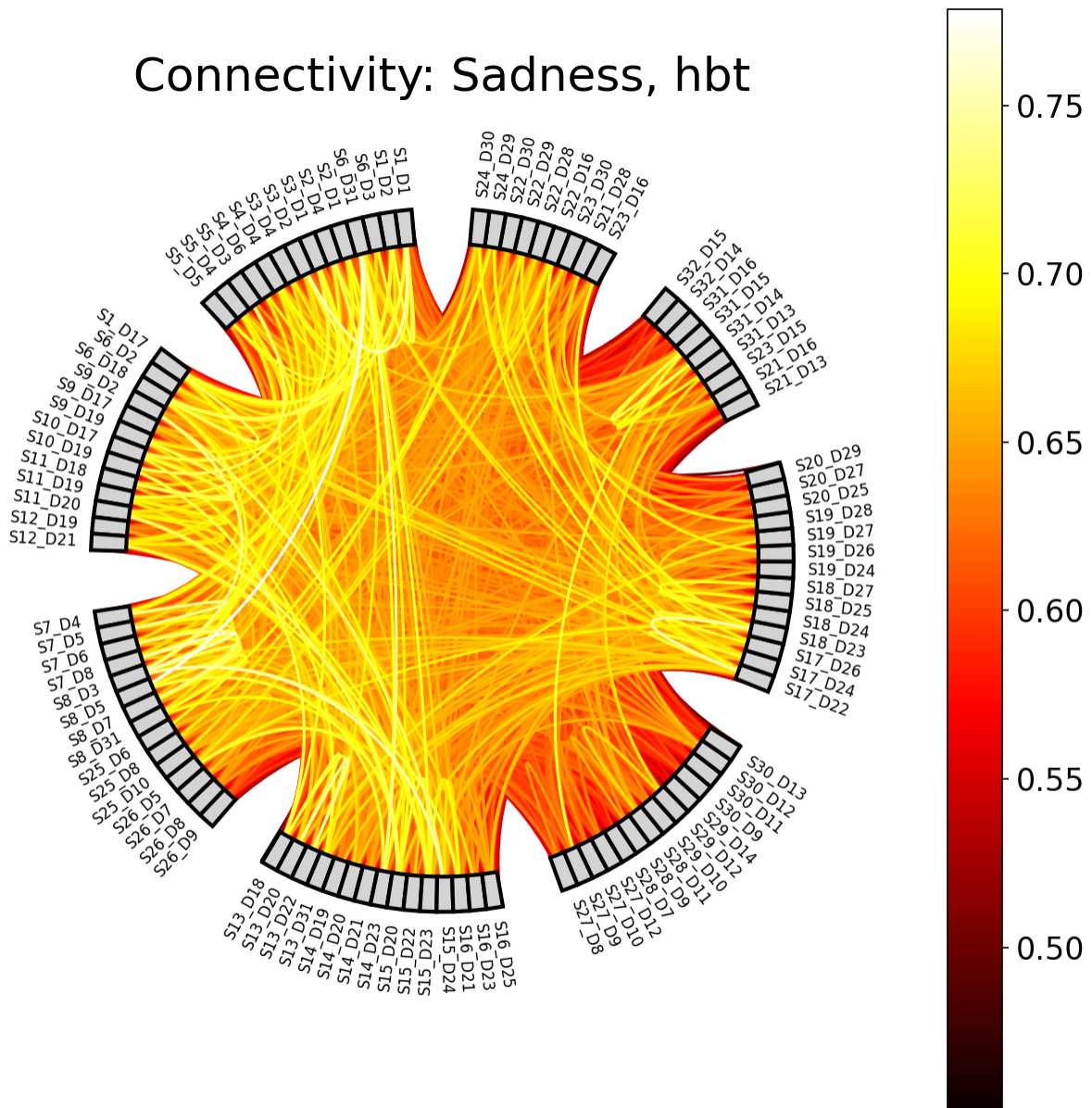


Figure 2.7: Example of a chord plot for the condition Sadness, showing the averaged connectivity across participants and epochs between 103 HbT channels (coherence values between 0 and 1). The color of the lines represents the coherence value. In general, the brighter the color, the stronger the connectivity between the two channels.

Paired Sample t-tests

For each mode (Face type/Emotion), and pair of conditions (e.g., Joy vs. Fear), individual-level connectivity matrices were extracted, averaging across epochs and time points to obtain, per participant, a symmetric channel-by-channel coherence matrix. Because co-

herence values are bounded between 0 and 1 and exhibit skewed distributions ([Miranda de Sá et al., 2009](#)), Fisher’s r-to-z transform (`atanh`) was applied to each matrix element to normalize the data prior to parametric testing. Paired t-tests for each unique channel pair ($i > j$) were then conducted across participants using SciPy’s `ttest_rel`. This directly tests whether mean connectivity differs between conditions, leveraging the paired design to increase statistical sensitivity ([Hu et al., 2023](#)). Given the large number of channel-pair tests, and similar to the GLM analysis above in [2.5.3](#), p -values were corrected for FDR using the Benjamini-Hochberg procedure ([Singh and Dan, 2006](#)) with a family-wise error rate of $\alpha=0.05$.

ROI Chord Plots

To distill high-dimensional channel-by-channel connectivity into interpretable inter-regional summaries, we mapped individual fNIRS channels onto anatomically defined ROI’s. This includes left and right frontal, prefrontal, parietal, occipital regions of the brain as shown in Figure [2.4](#), and the channels were grouped into these regions based on their location in the montage. Since multiple channels may map to the same pair of regions (e.g., several left prefrontal channels connecting to several right occipital channels), we aggregated all significant connections ($p < 0.05$) between two regions by taking the mean of their t-values.

2.5.5 Memory Task Analysis

Recall the memory task described in [2.3.1](#), where participants were asked to indicate whether the 9th face was in the previous block of 8 faces with a ‘yes’ or ‘no’ response on the keyboard. The memory task was not the main focus of the study, but it was used to keep the participants engaged and focused on the faces. However, one can investigate whether participants’ ability to correctly recognize or recall emotional facial expressions varied depending on the type of face (e.g., real vs. virtual) and the emotion

displayed (e.g., happy, sad, angry). Raw behavioral data files from the output of the PsychoPy presentation were systematically preprocessed to isolate key response variables. For example, if the participant pressed 'y' for yes, and the 9th face was indeed in the previous block, they answered correctly, and if they pressed 'y' for yes, and the 9th face was not in the previous block, they answered incorrectly. The same applies for the 'n' for no responses. The total correct trials per participant were then summed. This data is not subject to the same signal quality criteria as the fNIRS data that was described in 2.1, as it is not a physiological measure. Therefore, all 87 participants can be included in the analysis, regardless of their fNIRS signal quality. However, participants achieving fewer correct responses than 34/56 (e.g., 60% of trials) were excluded to ensure sufficient engagement in the task, as shown in Figure 2.8. Only one participant was excluded from the analysis.

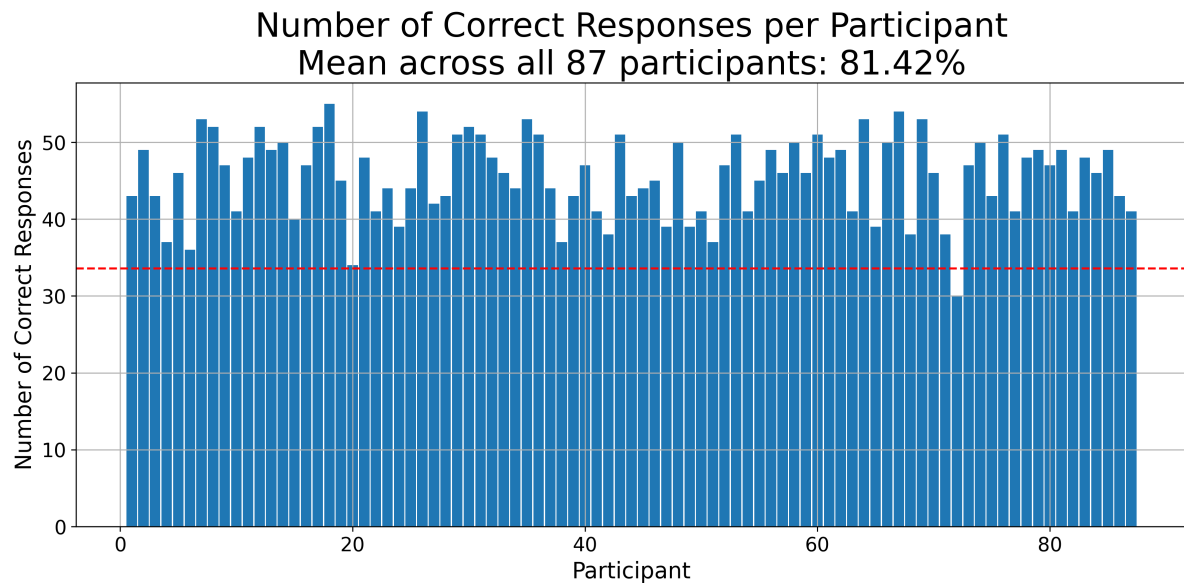


Figure 2.8: Number of correct responses by participant, the red dashed line represents the threshold of 34/56 correct responses (60%) that participants must meet to be included in the analysis. Only one participant was excluded from the analysis.

Since each block of faces was either all real or all virtual, and all had the same emotional expression (as discussed in 2.3.1), each y/n response was labeled with Face

type and Emotion. An OLS model was fit with accuracy (converted to numeric 0/1) as the dependent variable and categorical predictors for Face Type, Emotion, and their interaction. The goal is to determine the main effects of these two factors individually, as well as their interaction, on response accuracy. A two-way Type III ANOVA (via `sm.stats.anova_lm(model, typ=3)`) provided F -statistics and p -values for main effects and interaction. This version of the ANOVA is especially suitable when interactions are included in the model, as it calculates each effect after accounting for all other terms.

Chapter 3

Results

3.1 General Linear Model (GLM) Results

3.1.1 Face Type Contrasts

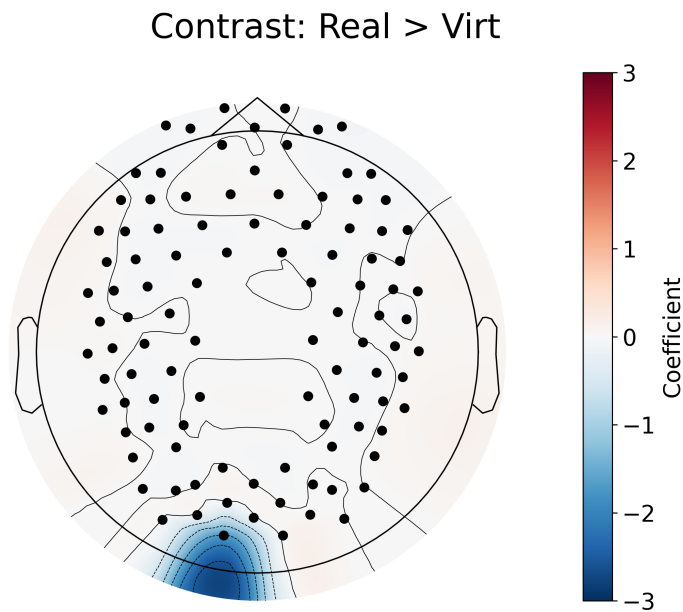


Figure 3.1: GLM contrast between real and virtual conditions which shows the differences in activation between the two conditions. Red signifies that condition 1 (real faces) has more activation in that area than condition 2 (virtual faces), while blue signifies that condition 2 (virtual faces) has more activation than condition 1 (real faces). The color bar on the right shows the coefficient of the contrast, which indicates the strength of the difference in activation between the two conditions.

The main effect of real versus virtual faces (as shown in 3.1) for the GLM revealed a significant difference in activation between real and virtual faces, with the left occipital channel showing greater activation for virtual faces compared to real faces.

3.1.2 Emotion Contrasts

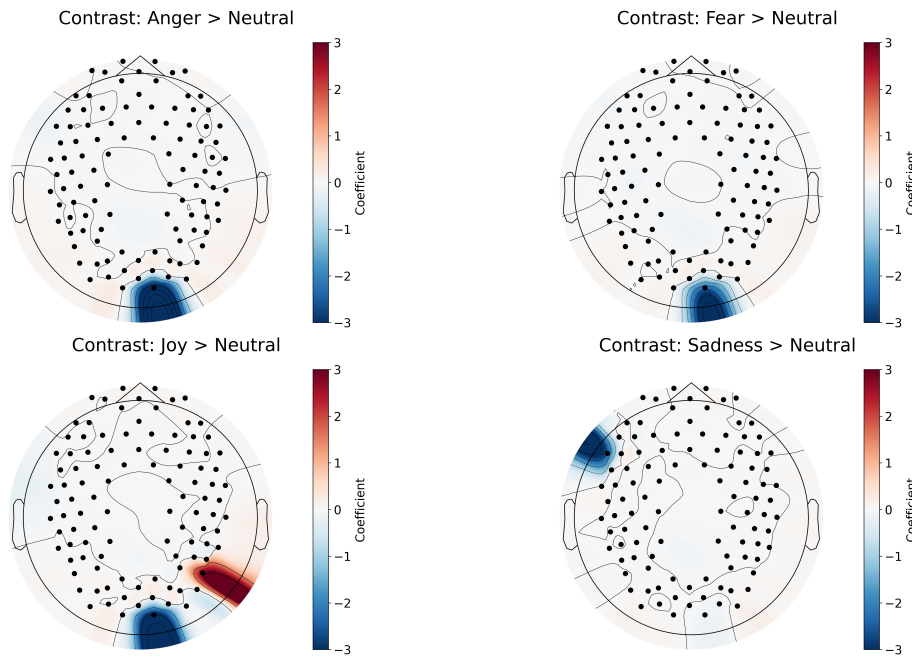


Figure 3.2: GLM results for the contrast between different emotions and neutral condition. Same concept as explained in figure 3.1.

Against the Neutral emotion (as shown in 3.2), the emotion contrasts revealed significant differences in activation across several brain regions. Specifically, Anger and Fear elicited greater activation in the right occipital region compared to Neutral. Joy was associated with increased activation in the right parietal region and decreased activation in the right occipital region, while sadness showed reduced activation in the left frontal region relative to Neutral. These results indicate distinct neural activation patterns for each emotion when contrasted with the Neutral baseline.

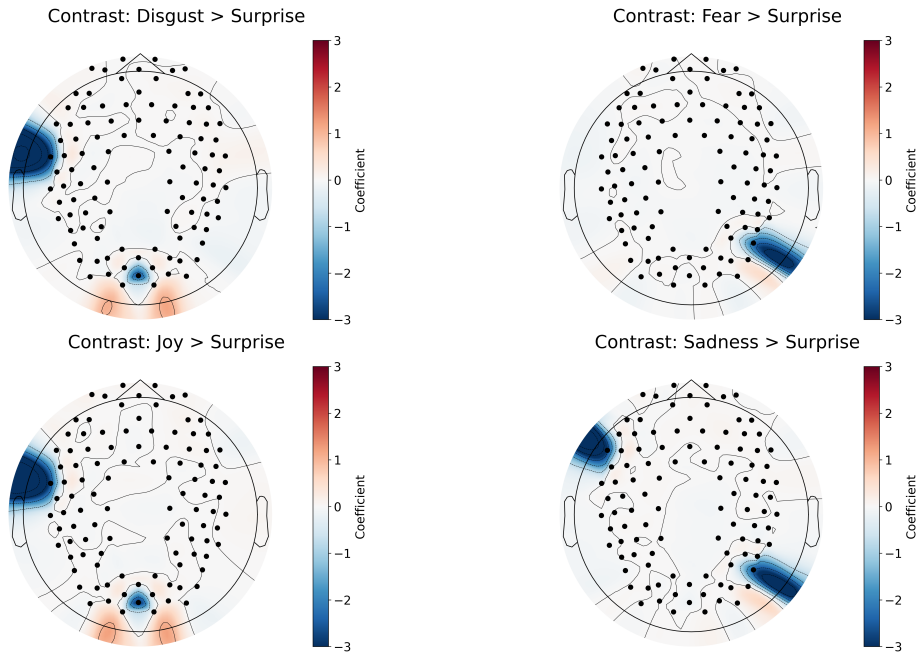


Figure 3.3: GLM results for the contrast between different emotions and surprise condition. Same concept as explained in figure 3.1.

When comparing each emotion against Surprise (as shown in 3.3), significant differences in activation were observed across multiple brain regions. Disgust and Joy both showed decreased activation in the right occipital and left prefrontal regions relative to Surprise. Fear was associated with reduced activation in the right parietal region, while Sadness showed decreased activation in both the left frontal and right parietal regions. These findings suggest that each emotion, when contrasted with Surprise, elicits distinct neural activation patterns all across the brain, rather than being limited to specific regions.

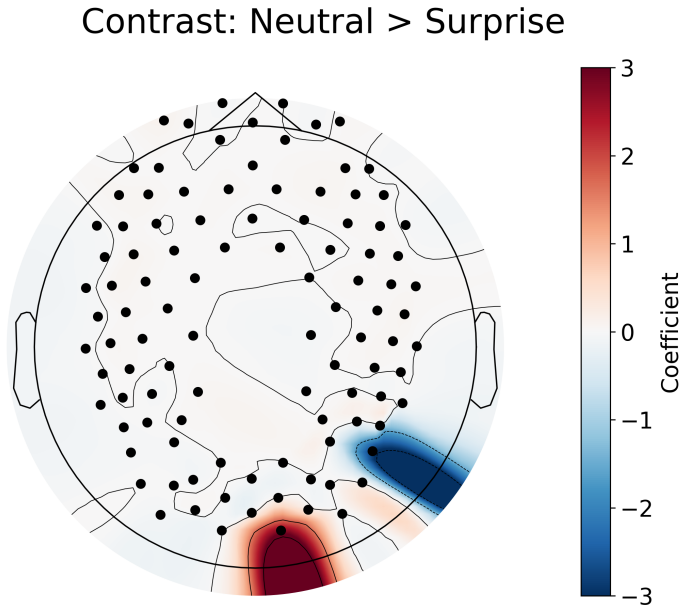


Figure 3.4: GLM results for the contrast between neutral and surprise condition. Same concept as explained in figure 3.1.

The Neutral > Surprise comparison (as shown in 3.4) revealed significant differences in the right parietal and right occipital regions. The right parietal region showed decreased activation (more activation for Surprise) while the right occipital region showed increased activation (more activation for neutral). Both Neutral and Surprise conditions elicit greater activation when compared to the other emotions, but when compared to each other, one emotion is not more activated than the other. This indicates that the neural response to Neutral and Surprise conditions is distinct, with each condition eliciting different activation patterns in specific brain regions. Note that all combinations of emotion contrasts were performed, no other significant differences were found between any other emotions than the ones shown in this section.

3.1.3 Face Type \times Emotion Contrasts

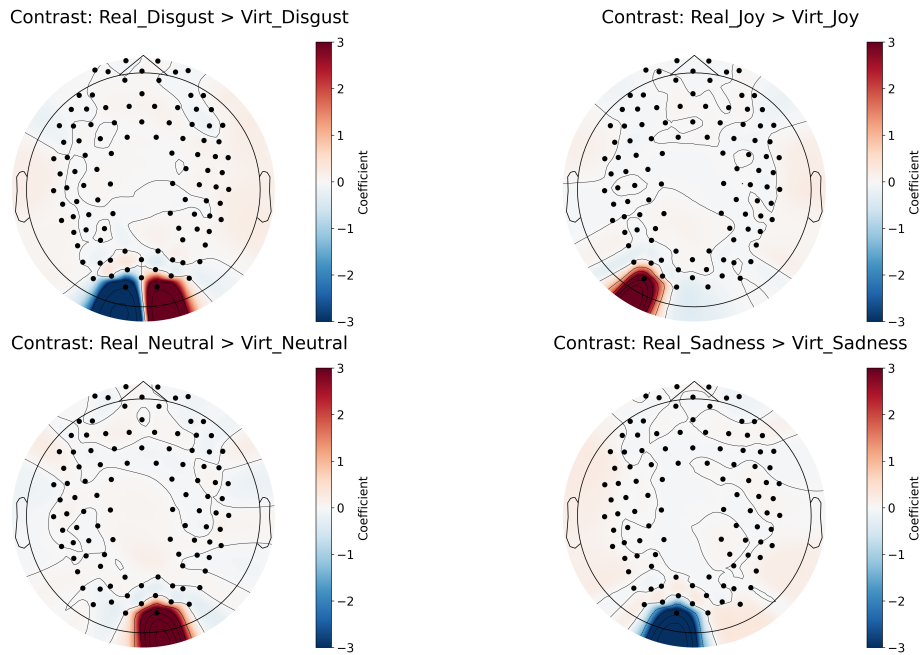


Figure 3.5: GLM results for the contrast between real and virtual conditions within each emotion. Same concept as explained in figure 3.1.

The interaction of face type with emotion (Real $>$ Virt within each emotion as shown in 3.5) revealed significant differences in occipital regions exclusively. In the case of disgust, real faces elicited greater activation in the right occipital region compared to virtual faces, while the left occipital region showed the opposite pattern. For Joy and Neutral emotions, real faces also elicited greater activation in the occipital regions compared to virtual faces. For Sadness, the left occipital region showed greater activation for virtual faces compared to real faces. These findings suggest that the neural response to emotional expressions is modulated by the realism of the face stimuli.

The full table of the GLM contrasts for all main effects and interactions can be found in Appendix A.

3.2 Functional Connectivity Results

3.2.1 Face Type Contrasts

Mean t-value by ROI: Real > Virt
 Mean t-value across ROI's: 1.55

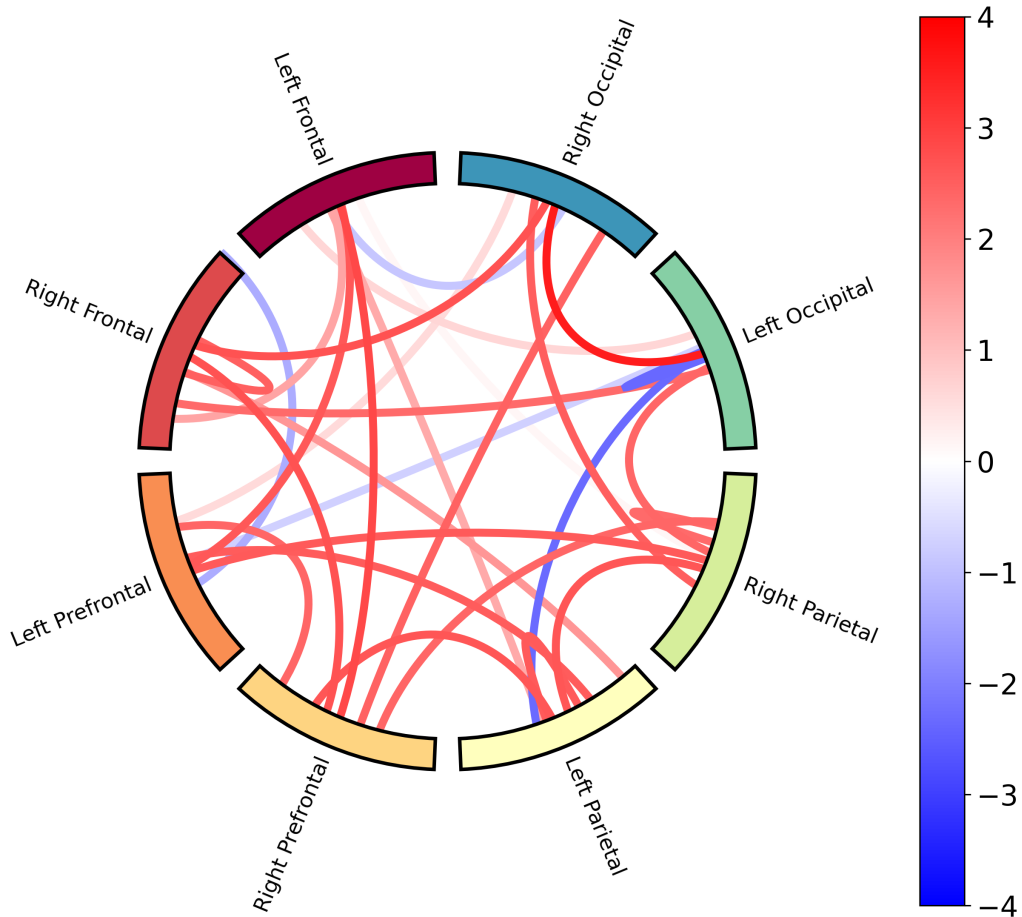


Figure 3.6: Functional connectivity results for the contrast between real and virtual conditions. Red signifies that condition 1 (real faces) has higher connectivity between those two ROI's than condition 2 (virtual faces), while blue signifies that condition 2 (virtual faces) has higher connectivity than condition 1 (real faces). The color bar on the right shows the t -statistic of the contrast, which indicates the strength of the difference in connectivity between the two conditions. The Mean t -value across ROI's is the average of the t -values for all significant channel pairs across all ROI's, and generally indicates whether the connectivity is higher or lower in one condition compared to the other. If this value is positive, it indicates that the connectivity is higher in condition 1 (real faces) than condition 2 (virtual faces), and vice versa.

The main effect of real versus virtual faces (as shown in 3.6) for functional connectivity revealed significant differences in connectivity between real and virtual faces across ROI's. Most ROI's showed higher connectivity for real faces compared to virtual faces, with a few exceptions, i.e. the left occipital/parietal ROI, which showed higher connectivity for virtual faces compared to real faces. A mean t -value of 1.55 indicates that the connectivity is generally higher for real faces compared to virtual faces across all ROI's.

3.2.2 Emotion Contrasts

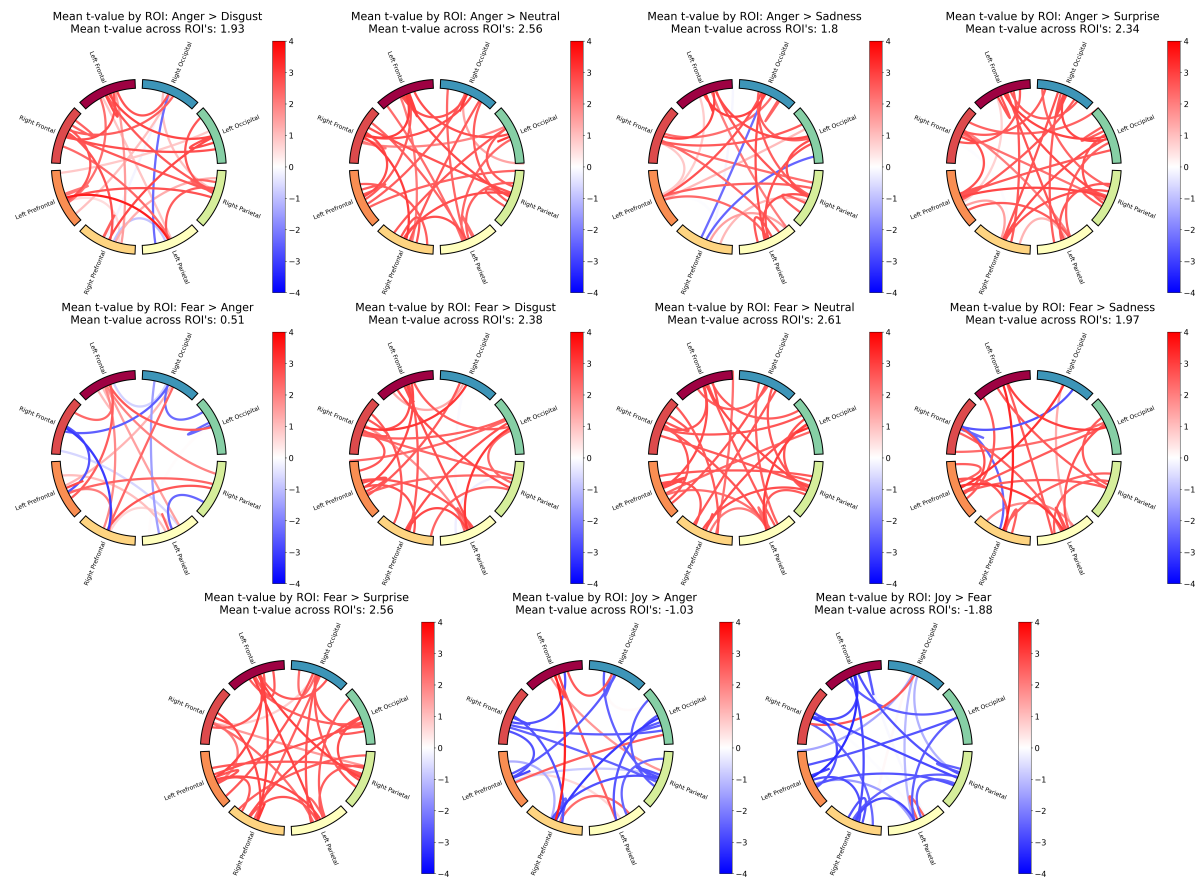


Figure 3.7: Functional connectivity results for Fear and Anger vs. the other emotions. Same concept as explained in figure 3.6.

The emotion contrasts (as shown in 3.7) revealed significant differences in functional connectivity across different emotions and ROI's. The t -values show that Anger and Fear showed higher connectivity in general compared to the other emotions, and when

compared to each other, Fear has only slightly higher connectivity than Anger. This higher connectivity for Anger and Fear as compared to the other emotions is consistent across most ROI's as well. The rest of the emotion contrasts can be found in Appendix B, which shows the remaining set of contrasts for all emotions.

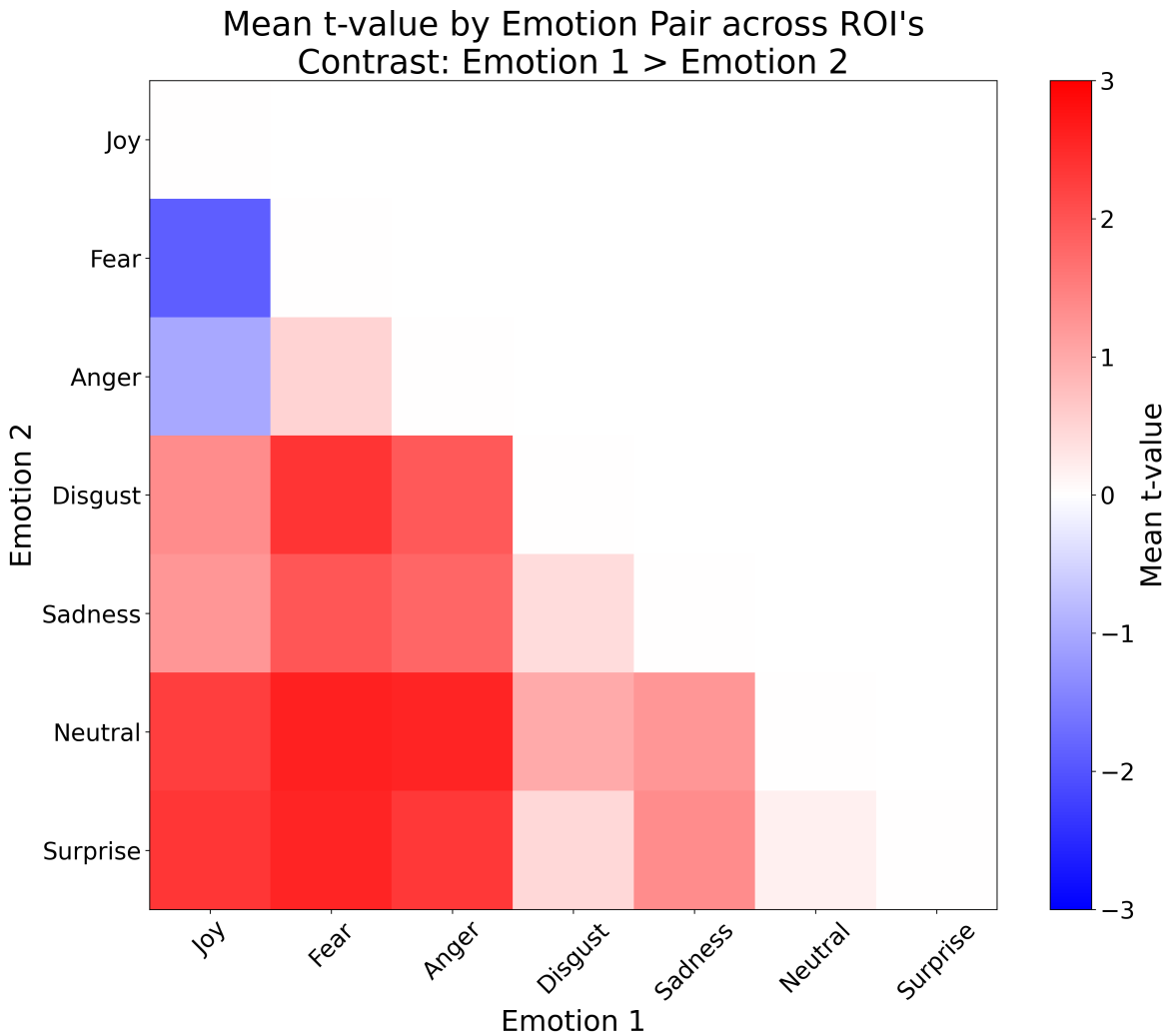


Figure 3.8: A heatmap summary of the functional connectivity results for the contrasts between different emotions. Red signifies that emotion 1 has higher connectivity than emotion 2, while blue signifies that emotion 2 has higher connectivity than emotion 1. The color bar on the right shows the t -value averaged across all significant channel pairs and across all ROI's, which indicates the strength of the difference in connectivity between the two emotions. This is the same value that is shown at the top of each plot in figure 3.6 and 3.7.

This summary of the functional connectivity results for the contrasts between different

emotions (as shown in 3.8) shows that Anger and Fear have the highest connectivity compared to the other emotions, with Fear having slightly higher connectivity than Anger. This lines up with figure 3.7, which shows that Anger and Fear have higher connectivity compared to the other emotions.

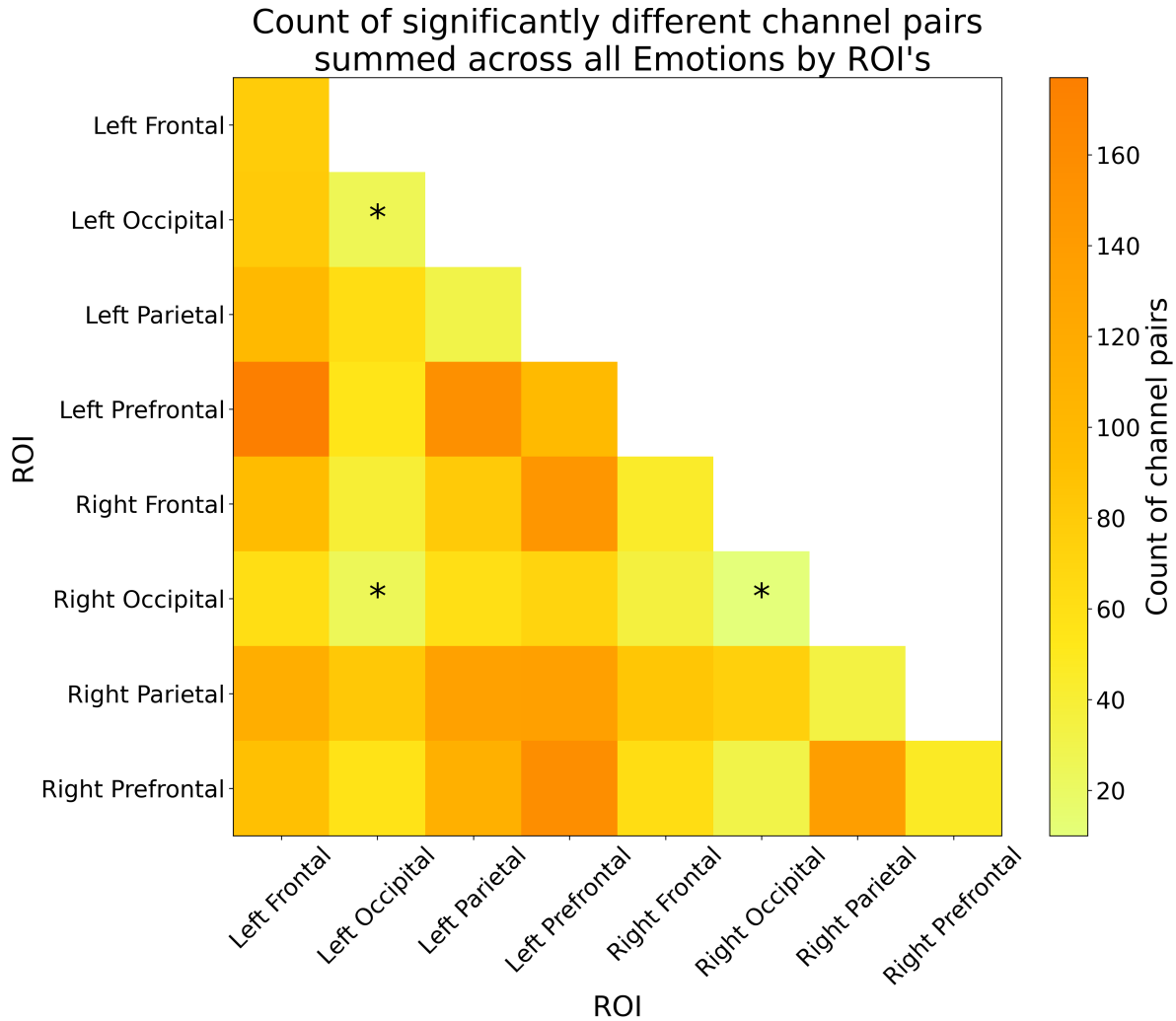


Figure 3.9: A heatmap summary of the number of significantly different channel pairs for each ROI summed across all emotions. The color bar on the right shows the number of significant channel pairs for each ROI, with brighter colors indicating a smaller number of significant channel pairs, and darker colors indicating a larger number of significant channel pairs. An asterisk was placed on the 3 ROI's with the least number of significantly different channel pairs to indicate that these ROI's are more synchronized with each other than any other pair of ROI's, regardless of the emotion. Note that ROI's can have differences within them, as each ROI is made up of multiple channels, and the differences are calculated between channels within the same ROI.

The count of significantly different channel pairs for each ROI summed across all emotions (as shown in 3.9) marks 3 regions with an asterisk, these regions have less channel pairs that are significantly different from each other, meaning that these regions are more synchronized with each other than any other pair of ROI's. These regions are the left occipital/right occipital, left occipital/left occipital, and right occipital/right occipital ROI's. This indicates that the differences in processing emotions occur in the frontal, prefrontal, and parietal regions of the brain.

3.2.3 Face Type \times Emotion Contrasts

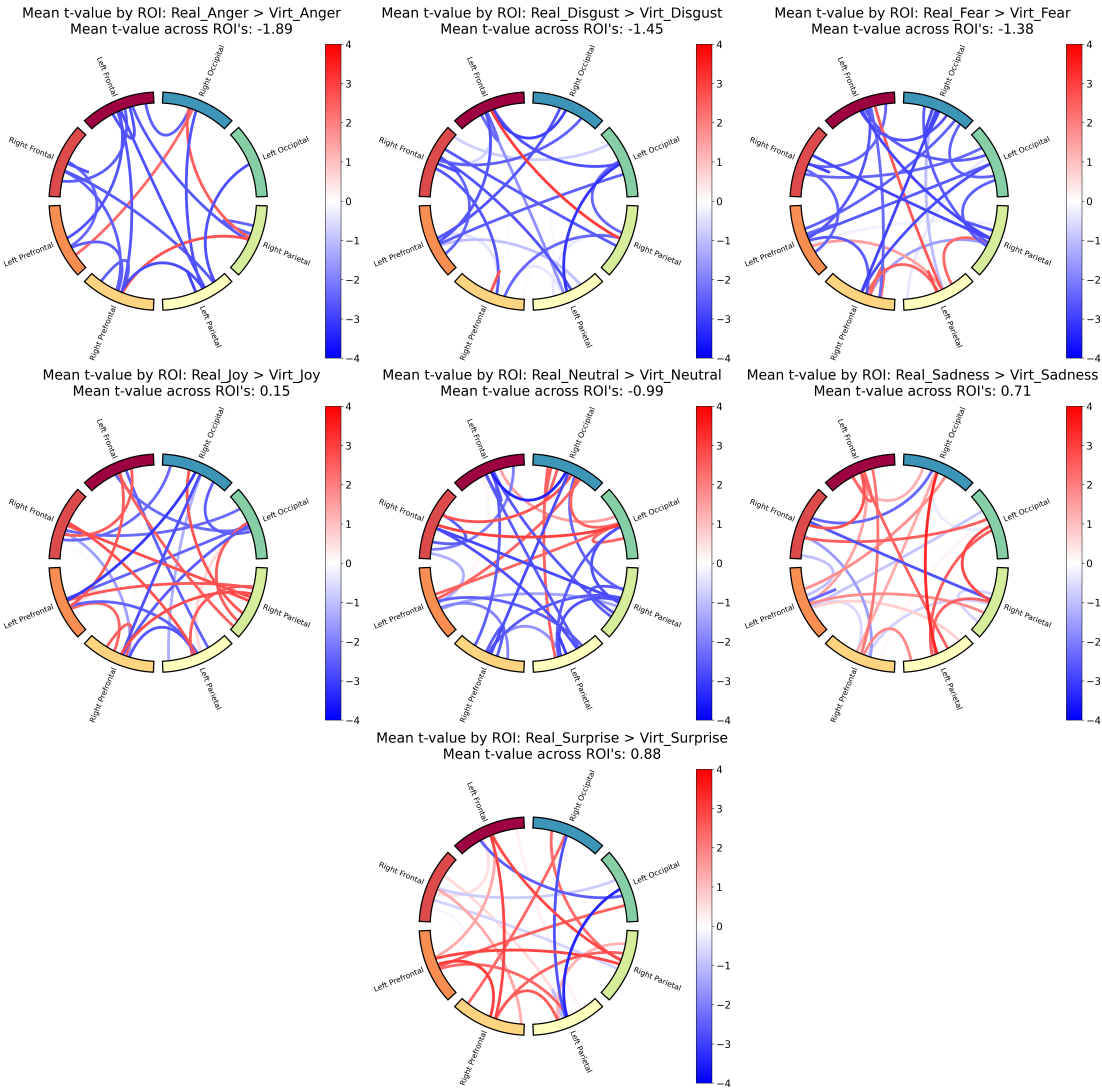


Figure 3.10: Functional connectivity results for the contrast between real and virtual conditions within each emotion. Same concept as explained in figure 3.6.

The interaction of face type with emotion (Real $>$ Virt within each emotion as shown in 3.10) revealed significant differences in functional connectivity across both face types within each emotion. For Anger, Disgust, Fear, and Neutral, virtual faces showed higher connectivity across most ROI's compared to real faces, whereas for Joy, Sadness, and Surprise, real faces showed higher connectivity across most ROI's compared to virtual faces. Like the GLM results, this indicates that the neural response to emotional expressions

is modulated by the realism of the face stimuli, with different patterns of connectivity observed for each face type \times emotion interaction.

The full table of the functional connectivity contrasts for all main effects and interactions can be found in Appendix B.

3.3 Memory Task Results

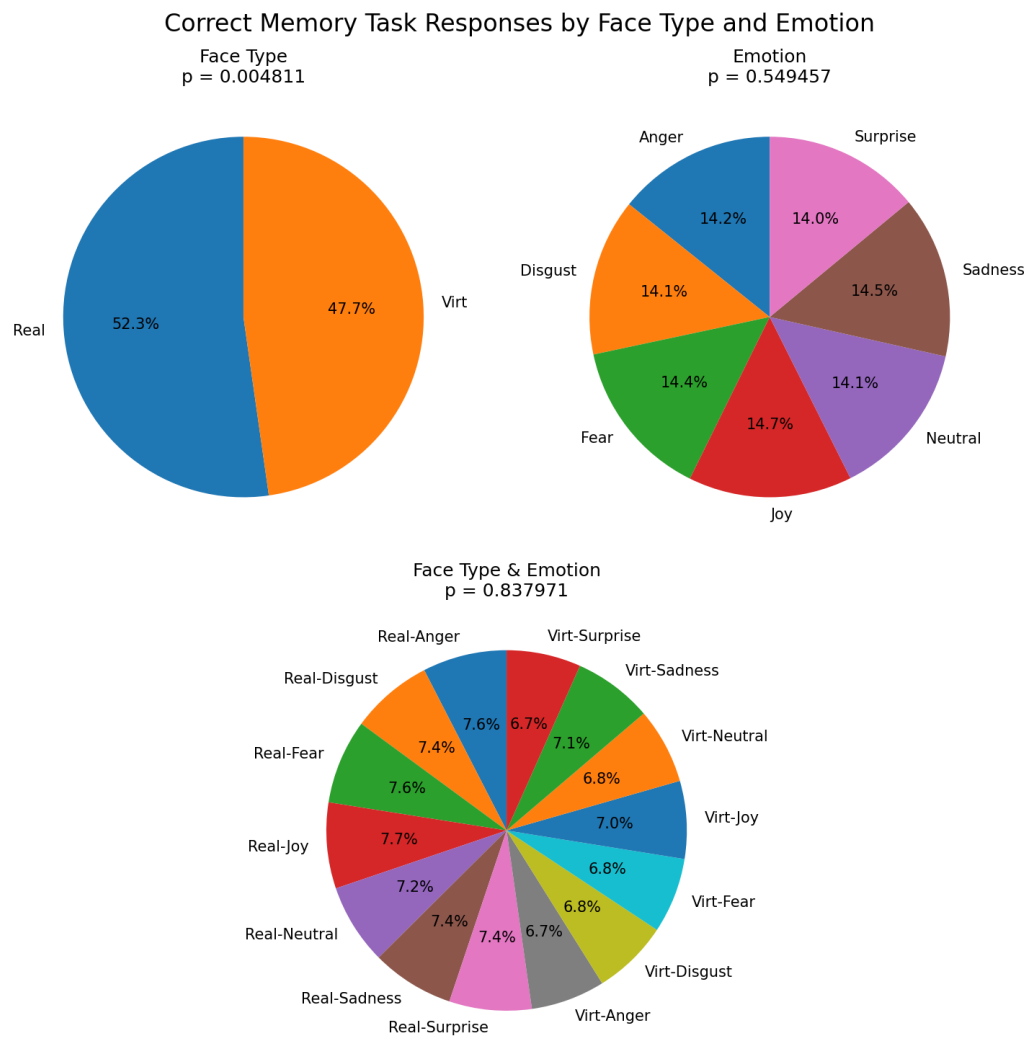


Figure 3.11: Proportion correct by condition in the memory task, plotted separately for real and virtual faces, for each emotion, and the interaction between face type and emotion. The p -values indicate the significance of the main effects and interaction.

A two-way Type III ANOVA (as described in 2.5.5) was conducted to examine the main effects and interaction on memory performance (proportion correct). Figure 3.11 shows accuracy by face type/emotion and their interaction. The analysis revealed a significant main effect of face type, $F(1, 4802) = 7.96, p = 0.0048$, indicating that memory performance was higher for real faces compared to virtual faces. There was no significant main effect of emotion, $F(6, 4802) = 0.83, p = 0.55$, nor a significant interaction between face type and emotion, $F(6, 4802) = 0.46, p = 0.84$. These findings suggest that while the realism of the face influences memory performance, the specific emotional expression does not have a significant impact on memory accuracy. The full ANOVA table is shown in Appendix C.

Chapter 4

Discussion

4.1 Limitations and Future Directions

4.2 Conclusion

Bibliography

- Bastos, A. M. and Schoffelen, J.-M. (2016). A Tutorial Review of Functional Connectivity Analysis Methods and Their Interpretational Pitfalls. *Frontiers in Systems Neuroscience*, 9. Publisher: Frontiers.
- Bergmann, T., Froese, L., Gomez, A., Sainbhi, A. S., Vakitbilir, N., Islam, A., Stein, K., Marquez, I., Amenta, F., Park, K., Ibrahim, Y., and Zeiler, F. A. (2023). Evaluation of Morlet Wavelet Analysis for Artifact Detection in Low-Frequency Commercial Near-Infrared Spectroscopy Systems. *Bioengineering*, 11(1):0.
- Bulgarelli, C., Blasi, A., McCann, S., Milosavljevic, B., Ghillia, G., Mbye, E., Touray, E., Fadera, T., Acolatse, L., Moore, S. E., Lloyd-Fox, S., Elwell, C. E., Eggebrecht, A. T., and Team, t. B. S. (2025). Growth in early infancy drives optimal brain functional connectivity which predicts cognitive flexibility in later childhood. Pages: 2024.01.02.573930 Section: New Results.
- Conley, M. I., Dellarco, D. V., Rubien-Thomas, E., Cohen, A. O., Cervera, A., Tottenham, N., and Casey, B. (2018). The racially diverse affective expression (RADIATE) face stimulus set. *Psychiatry Research*, 270:1059–1067.
- Cui, X., Bray, S., and Reiss, A. L. (2010). Functional near infrared spectroscopy (NIRS) signal improvement based on negative correlation between oxygenated and deoxygenated hemoglobin dynamics. *NeuroImage*, 49(4):3039–3046.

- Ekman, P. (1992). Are there basic emotions? *Psychological Review*, 99(3):550–553. Place: US Publisher: American Psychological Association.
- Ekman, P. and Friesen, W. V. (1978). Facial action coding system. *Environmental Psychology & Nonverbal Behavior*.
- Fishburn, F. A., Ludlum, R. S., Vaidya, C. J., and Medvedev, A. V. (2019). Temporal Derivative Distribution Repair (TDDR): A motion correction method for fNIRS. *NeuroImage*, 184:171–179.
- Friston, K. J. (2007). *Statistical parametric mapping: the analysis of functional brain images*. Elsevier / Academic Press, Amsterdam Boston, 1st ed edition.
- Gramfort, A., Luessi, M., Larson, E., Engemann, D. A., Strohmeier, D., Brodbeck, C., Goj, R., Jas, M., Brooks, T., Parkkonen, L., and Hämäläinen, M. (2013). MEG and EEG data analysis with MNE-Python. *Frontiers in Neuroscience*, 7. Publisher: Frontiers.
- Hakim, U., De Felice, S., Pinti, P., Zhang, X., Noah, J., Ono, Y., Burgess, P. W., Hamilton, A., Hirsch, J., and Tachtsidis, I. (2023). Quantification of inter-brain coupling: A review of current methods used in haemodynamic and electrophysiological hyperscanning studies. *NeuroImage*, 280:120354.
- Hernandez, S. M. and Pollonini, L. (2020). NIRSpot: A Tool for Quality Assessment of fNIRS Scans. In *Biophotonics Congress: Biomedical Optics 2020 (Translational, Microscopy, OCT, OTS, BRAIN)*, page BM2C.5, Washington, DC. Optica Publishing Group.
- Hocke, L. M., Oni, I. K., Duszynski, C. C., Corrigan, A. V., Frederick, B. D., and Dunn, J. F. (2018). Automated Processing of fNIRS Data—A Visual Guide to the Pitfalls and Consequences. *Algorithms*, 11(5):67. Number: 5 Publisher: Multidisciplinary Digital Publishing Institute.

- Holmes, M., Aalto, D., and Cummine, J. (2024). Opening the dialogue: A preliminary exploration of hair color, hair cleanliness, light, and motion effects on fNIRS signal quality. *PLOS ONE*, 19(5):e0304356. Publisher: Public Library of Science.
- Hu, P., Wang, P., Zhao, R., Yang, H., and Biswal, B. B. (2023). Characterizing the spatiotemporal features of functional connectivity across the white matter and gray matter during the naturalistic condition. *Frontiers in Neuroscience*, 17. Publisher: Frontiers.
- Kinder, K. T., Heim, H. L. R., Parker, J., Lowery, K., McCraw, A., Eddings, R. N., Defenderfer, J., Sullivan, J., and Buss, A. T. (2022). Systematic review of fNIRS studies reveals inconsistent chromophore data reporting practices. *Neurophotonics*, 9(4):040601.
- Kocsis, L., Herman, P., and Eke, A. (2006). The modified Beer–Lambert law revisited. *Physics in Medicine & Biology*, 51(5):N91.
- Lindquist, K. A., Wager, T. D., Kober, H., Bliss-Moreau, E., and Barrett, L. F. (2012). The brain basis of emotion: A meta-analytic review. *Behavioral and Brain Sciences*, 35(3):121–143.
- Luke, R., Larson, E. D., Shader, M. J., Innes-Brown, H., Yper, L. V., Lee, A. K. C., Sowman, P. F., and McAlpine, D. (2021). Analysis methods for measuring passive auditory fNIRS responses generated by a block-design paradigm. *Neurophotonics*, 8(2):025008. Publisher: SPIE.
- Miranda de Sá, A. M. F. L., Ferreira, D. D., Dias, E. W., Mendes, E. M. A. M., and Felix, L. B. (2009). Coherence estimate between a random and a periodic signal: Bias, variance, analytical critical values, and normalizing transforms. *Journal of the Franklin Institute*, 346(9):841–853.

- Oliver, M. M. and Amengual Alcover, E. (2020). UIBVFED: Virtual facial expression dataset. *PLOS ONE*, 15(4):e0231266.
- Peirce, J., Gray, J. R., Simpson, S., MacAskill, M., Höchenberger, R., Sogo, H., Kastman, E., and Lindeløv, J. K. (2019). PsychoPy2: Experiments in behavior made easy. *Behavior Research Methods*, 51(1):195–203.
- Pinti, P., Scholkmann, F., Hamilton, A., Burgess, P., and Tachtsidis, I. (2019). Current Status and Issues Regarding Pre-processing of fNIRS Neuroimaging Data: An Investigation of Diverse Signal Filtering Methods Within a General Linear Model Framework. *Frontiers in Human Neuroscience*, 12.
- Pollonini, L., Bortfeld, H., and Oghalai, J. S. (2016). PHOEBE: a method for real time mapping of optodes-scalp coupling in functional near-infrared spectroscopy. *Biomedical Optics Express*, 7(12):5104–5119. Publisher: Optica Publishing Group.
- Reddy, P., Izzetoglu, M., Shewokis, P. A., Sangobowale, M., Diaz-Arrastia, R., and Izzetoglu, K. (2021). Evaluation of fNIRS signal components elicited by cognitive and hypercapnic stimuli. *Scientific Reports*, 11(1):23457. Publisher: Nature Publishing Group.
- Scholkmann, F., Metz, A. J., and Wolf, M. (2014). Measuring tissue hemodynamics and oxygenation by continuous-wave functional near-infrared spectroscopy—how robust are the different calculation methods against movement artifacts? *Physiological Measurement*, 35(4):717. Publisher: IOP Publishing.
- Singh, A. K. and Dan, I. (2006). Exploring the false discovery rate in multichannel NIRS. *NeuroImage*, 33(2):542–549.
- Tachtsidis, I. and Scholkmann, F. (2016). False positives and false negatives in functional near-infrared spectroscopy: issues, challenges, and the way forward. *Neurophotonics*, 3(3):031405. Publisher: SPIE.

Xu, G., Zhang, M., Wang, Y., Liu, Z., Huo, C., Li, Z., and Huo, M. (2017). Functional connectivity analysis of distracted drivers based on the wavelet phase coherence of functional near-infrared spectroscopy signals. *PLOS ONE*, 12(11):e0188329. Publisher: Public Library of Science.

Appendix A

GLM Contrasts

Table A.1: Table of contrast results from the GLM analysis.

Contrast	Region	Ch Name	Coef.	Std.Err.	<i>z</i>	<i>p_{fdr}</i>
Real > Virt	Left Occipital	S23 D15 hbt	-1.550	0.394	-3.937	0.009
Joy > Neutral	Right Parietal	S20 D29 hbt	2.611	0.623	4.194	0.001
Joy > Neutral	Right Occipital	S23 D30 hbt	-3.144	0.623	-5.050	0.000
Joy > Surprise	Right Occipital	S23 D16 hbt	-2.884	0.647	-4.460	0.001
Joy > Surprise	Left Prefrontal	S25 D6 hbt	-2.379	0.647	-3.679	0.012
Fear > Neutral	Right Occipital	S23 D30 hbt	-2.126	0.557	-3.819	0.014
Fear > Surprise	Right Parietal	S20 D29 hbt	-2.048	0.568	-3.606	0.032
Anger > Neutral	Right Occipital	S23 D30 hbt	-3.620	0.652	-5.547	0.000
Disgust > Surprise	Right Occipital	S23 D16 hbt	-2.507	0.640	-3.920	0.005
Disgust > Surprise	Left Prefrontal	S25 D6 hbt	-2.531	0.640	-3.958	0.005
Sadness > Neutral	Left Frontal	S4 D6 hbt	-2.257	0.601	-3.754	0.018
Sadness > Surprise	Left Frontal	S4 D6 hbt	-2.610	0.673	-3.879	0.011
Sadness > Surprise	Right Parietal	S20 D29 hbt	-2.304	0.673	-3.425	0.032

Continued on next page

Table A.1: Table of contrast results from the GLM analysis.

Contrast	Region	Ch Name	Coef.	Std.Err.	<i>z</i>	<i>p</i> _{fdr}
Neutral > Surprise	Right Parietal	S20 D29 hbt	-2.653	0.625	-4.247	0.002
Neutral > Surprise	Right Occipital	S23 D30 hbt	2.461	0.625	3.940	0.004
Real Joy > Real Disgust	Right Occipital	S23 D30 hbt	-5.344	1.093	-4.889	0.000
Real Joy > Real Sadness	Right Occipital	S24 D30 hbt	-3.816	0.964	-3.958	0.008
Real Joy > Real Neutral	Right Occipital	S23 D30 hbt	-5.786	0.980	-5.906	0.000
Real Joy > Real Surprise	Right Frontal	S9 D19 hbt	3.093	0.997	3.101	0.050
Real Joy > Real Surprise	Left Occipital	S23 D15 hbt	-3.754	0.997	-3.764	0.017
Real Joy > Real Surprise	Right Occipital	S23 D16 hbt	-3.577	0.997	-3.587	0.017
Real Joy > Real Surprise	Left Prefrontal	S25 D6 hbt	-3.293	0.997	-3.302	0.033
Real Joy > Virt Joy	Left Occipital	S32 D15 hbt	3.484	0.966	3.607	0.032
Real Joy > Virt Fear	Left Occipital	S23 D15 hbt	-3.384	0.965	-3.506	0.023
Real Joy > Virt Fear	Right Occipital	S23 D30 hbt	-3.649	0.965	-3.781	0.016
Real Joy > Virt Disgust	Left Occipital	S23 D15 hbt	-4.428	0.986	-4.490	0.001
Real Joy > Virt Sadness	Left Occipital	S23 D15 hbt	-4.435	0.973	-4.556	0.001
Real Joy > Virt Surprise	Right Occipital	S23 D16 hbt	-3.197	0.949	-3.368	0.039
Real Joy > Virt Surprise	Right Occipital	S23 D30 hbt	-3.410	0.949	-3.593	0.034
Real Fear > Real Disgust	Right Occipital	S23 D30 hbt	-4.918	1.087	-4.522	0.001
Real Fear > Real Neutral	Right Occipital	S23 D30 hbt	-5.360	0.980	-5.470	0.000
Real Fear > Virt Joy	Left Prefrontal	S25 D6 hbt	4.150	1.054	3.938	0.008
Real Fear > Virt Disgust	Left Occipital	S23 D15 hbt	-4.112	1.009	-4.073	0.002
Real Fear > Virt Disgust	Left Prefrontal	S25 D6 hbt	4.183	1.009	4.144	0.002
Real Fear > Virt Sadness	Left Occipital	S23 D15 hbt	-4.119	1.003	-4.109	0.004
Real Fear > Virt Sadness	Left Prefrontal	S25 D6 hbt	3.595	1.003	3.585	0.017

Continued on next page

Table A.1: Table of contrast results from the GLM analysis.

Contrast	Region	Ch Name	Coef.	Std.Err.	<i>z</i>	<i>p</i> _{fdr}
Real Anger > Real Disgust	Right Occipital	S23 D30 hbt	-4.697	1.117	-4.205	0.003
Real Anger > Real Neutral	Right Occipital	S23 D30 hbt	-5.139	0.983	-5.226	0.000
Real Disgust > Real Surprise	Left Frontal	S4 D6 hbt	-3.742	1.107	-3.380	0.025
Real Disgust > Real Surprise	Left Occipital	S23 D15 hbt	-4.679	1.107	-4.226	0.002
Real Disgust > Real Surprise	Right Occipital	S23 D30 hbt	4.221	1.107	3.813	0.007
Real Disgust > Virt Fear	Left Occipital	S23 D15 hbt	-4.309	1.013	-4.252	0.002
Real Disgust > Virt Disgust	Left Occipital	S23 D15 hbt	-5.353	1.163	-4.603	0.000
Real Disgust > Virt Disgust	Right Occipital	S23 D30 hbt	5.028	1.163	4.323	0.001
Real Disgust > Virt Sadness	Left Occipital	S23 D15 hbt	-5.360	1.163	-4.608	0.000
Real Disgust > Virt Sadness	Right Occipital	S23 D30 hbt	4.254	1.163	3.657	0.013
Real Disgust > Virt Neutral	Right Occipital	S23 D30 hbt	3.878	1.102	3.520	0.044
Real Sadness > Real Neutral	Right Occipital	S23 D30 hbt	-3.749	0.912	-4.110	0.002
Real Sadness > Real Neutral	Right Occipital	S24 D30 hbt	4.012	0.912	4.398	0.001
Real Sadness > Real Surprise	Left Frontal	S4 D6 hbt	-3.743	1.059	-3.534	0.021
Real Sadness > Real Surprise	Right Occipital	S24 D30 hbt	4.688	1.059	4.426	0.001
Real Sadness > Virt Joy	Right Occipital	S24 D30 hbt	3.811	1.048	3.638	0.028
Real Sadness > Virt Disgust	Left Occipital	S23 D15 hbt	-3.951	1.088	-3.633	0.029
Real Sadness > Virt Sadness	Left Occipital	S23 D15 hbt	-3.959	1.051	-3.766	0.017
Real Neutral > Real Surprise	Right Parietal	S20 D29 hbt	-3.553	0.933	-3.809	0.007
Real Neutral > Real Surprise	Right Occipital	S23 D30 hbt	4.663	0.933	4.999	0.000
Real Neutral > Virt Joy	Right Occipital	S23 D30 hbt	3.563	0.924	3.856	0.012
Real Neutral > Virt Anger	Left Frontal	S4 D6 hbt	4.371	1.009	4.330	0.002
Real Neutral > Virt Anger	Right Occipital	S23 D30 hbt	3.737	1.009	3.702	0.011

Continued on next page

Table A.1: Table of contrast results from the GLM analysis.

Contrast	Region	Ch Name	Coef.	Std.Err.	<i>z</i>	<i>p</i> _{fdr}
Real Neutral > Virt Disgust	Right Occipital	S23 D30 hbt	5.470	1.020	5.365	0.000
Real Neutral > Virt Sadness	Left Frontal	S4 D6 hbt	4.863	0.963	5.051	0.000
Real Neutral > Virt Sadness	Right Occipital	S23 D30 hbt	4.696	0.963	4.877	0.000
Real Neutral > Virt Neutral	Right Occipital	S23 D30 hbt	4.320	0.994	4.346	0.001
Real Surprise > Virt Joy	Left Frontal	S4 D6 hbt	3.580	1.038	3.448	0.029
Real Surprise > Virt Joy	Left Prefrontal	S25 D6 hbt	4.185	1.038	4.030	0.006
Real Surprise > Virt Anger	Left Frontal	S4 D6 hbt	5.443	1.096	4.966	0.000
Real Surprise > Virt Anger	Right Frontal	S10 D17 hbt	-3.659	1.096	-3.338	0.029
Real Surprise > Virt Anger	Left Occipital	S23 D15 hbt	3.907	1.096	3.565	0.019
Real Surprise > Virt Disgust	Left Prefrontal	S25 D6 hbt	4.218	1.042	4.048	0.005
Real Surprise > Virt Sadness	Left Frontal	S4 D6 hbt	5.935	1.000	5.937	0.000
Real Surprise > Virt Sadness	Left Prefrontal	S7 D6 hbt	3.660	1.000	3.661	0.007
Real Surprise > Virt Sadness	Right Parietal	S20 D29 hbt	4.101	1.000	4.102	0.002
Real Surprise > Virt Sadness	Left Prefrontal	S25 D6 hbt	3.630	1.000	3.631	0.007
Real Surprise > Virt Neutral	Left Frontal	S4 D6 hbt	3.189	1.025	3.111	0.048
Real Surprise > Virt Neutral	Right Frontal	S9 D19 hbt	-3.357	1.025	-3.275	0.048
Real Surprise > Virt Neutral	Right Parietal	S20 D29 hbt	3.539	1.025	3.453	0.048
Real Surprise > Virt Neutral	Left Occipital	S31 D15 hbt	-3.254	1.025	-3.174	0.048
Virt Joy > Virt Disgust	Left Occipital	S32 D15 hbt	-4.343	1.008	-4.308	0.002
Virt Fear > Virt Disgust	Right Occipital	S23 D30 hbt	3.333	0.928	3.590	0.034
Virt Fear > Virt Sadness	Left Frontal	S4 D6 hbt	3.597	1.021	3.522	0.044
Virt Anger > Virt Disgust	Left Frontal	S4 D6 hbt	-3.633	1.033	-3.518	0.019
Virt Anger > Virt Disgust	Left Occipital	S23 D15 hbt	-4.581	1.033	-4.436	0.001

Continued on next page

Table A.1: Table of contrast results from the GLM analysis.

Contrast	Region	Ch Name	Coef.	Std.Err.	<i>z</i>	<i>p</i> _{fdr}
Virt Anger > Virt Disgust	Left Prefrontal	S25 D6 hbt	3.565	1.033	3.452	0.019
Virt Anger > Virt Sadness	Left Occipital	S23 D15 hbt	-4.589	1.018	-4.508	0.001
Virt Disgust > Virt Sadness	Left Frontal	S4 D6 hbt	4.125	1.044	3.950	0.008
Virt Disgust > Virt Surprise	Left Occipital	S23 D15 hbt	3.761	1.001	3.758	0.018
Virt Sadness > Virt Surprise	Left Occipital	S23 D15 hbt	3.768	0.978	3.853	0.012

Appendix B

Functional Connectivity Contrasts

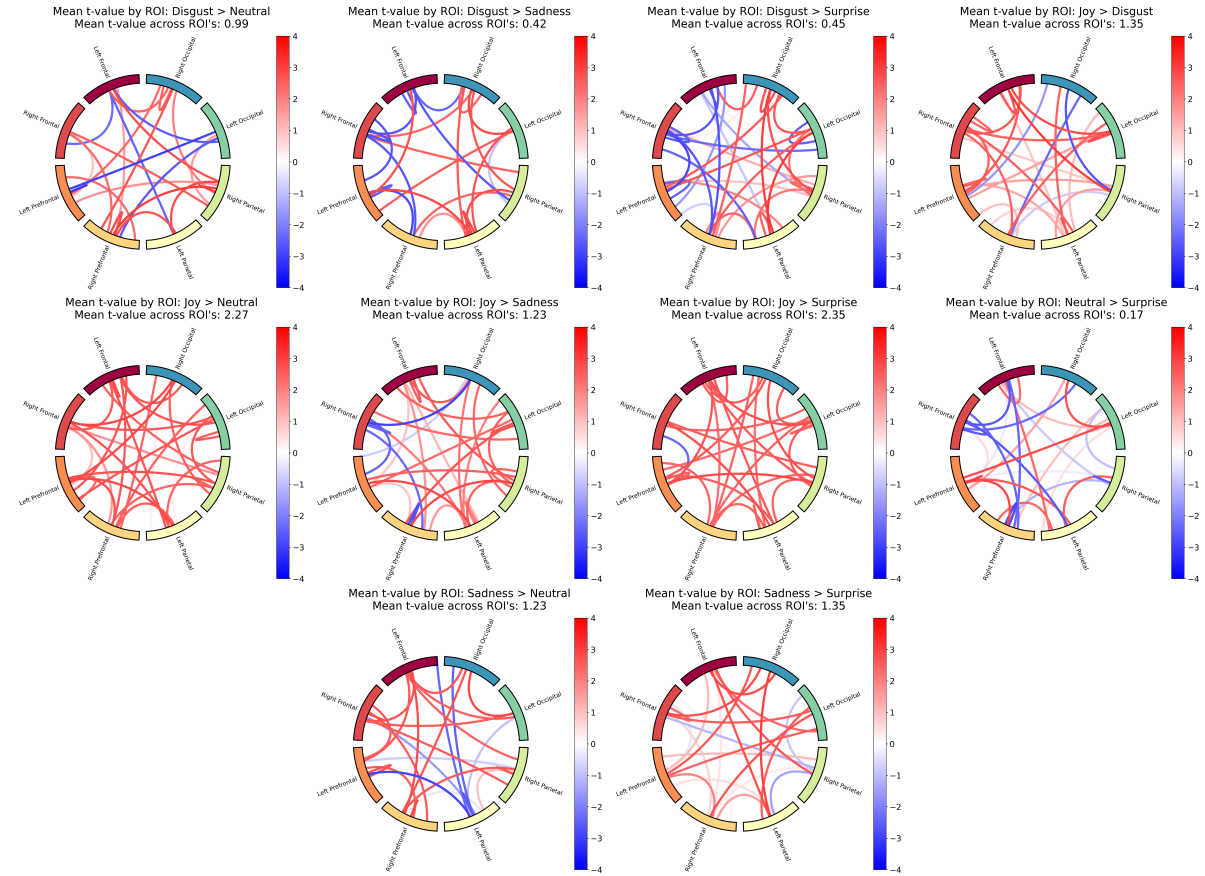


Figure B.1: Functional connectivity results for the rest of the contrasts. Same concept as explained in figure 3.6. These are the rest of the contrasts that were not shown in 3.7.

Table B.1: Group level t -tests and Sum of Significantly different channels averaged across ROIs.

Contrast	Mean t value	Sum of Sig. diff channels
Real > Virt	1.546	114.000
Joy > Fear	-1.880	118.000
Joy > Anger	-1.025	65.000
Joy > Disgust	1.354	135.000
Joy > Sadness	1.229	127.000
Joy > Neutral	2.269	113.000
Joy > Surprise	2.346	84.000
Fear > Anger	0.511	113.000
Fear > Disgust	2.382	196.000
Fear > Sadness	1.975	89.000
Fear > Neutral	2.615	263.000
Fear > Surprise	2.558	290.000
Anger > Disgust	1.929	164.000
Anger > Sadness	1.797	158.000
Anger > Neutral	2.565	185.000
Anger > Surprise	2.335	194.000
Disgust > Sadness	0.415	71.000
Disgust > Neutral	0.994	93.000
Disgust > Surprise	0.447	128.000
Sadness > Neutral	1.232	90.000
Sadness > Surprise	1.352	100.000
Neutral > Surprise	0.172	104.000

Continued on next page

Table B.1: Group level t -tests and Sum of Significantly different channels averaged across ROIs.

Contrast	Mean t value	Sum of Sig. diff channels
Real Joy > Real Fear	-0.243	109.000
Real Joy > Real Anger	-1.058	97.000
Real Joy > Real Disgust	2.089	84.000
Real Joy > Real Sadness	-0.986	154.000
Real Joy > Real Neutral	1.012	201.000
Real Joy > Real Surprise	0.676	124.000
Real Joy > Virt Joy	0.148	130.000
Real Joy > Virt Fear	-2.114	136.000
Real Joy > Virt Anger	-2.618	132.000
Real Joy > Virt Disgust	-1.637	99.000
Real Joy > Virt Sadness	0.285	93.000
Real Joy > Virt Neutral	0.204	76.000
Real Joy > Virt Surprise	1.456	117.000
Real Fear > Real Anger	-0.969	126.000
Real Fear > Real Disgust	1.906	119.000
Real Fear > Real Sadness	0.270	61.000
Real Fear > Real Neutral	1.413	167.000
Real Fear > Real Surprise	0.687	110.000
Real Fear > Virt Joy	0.371	129.000
Real Fear > Virt Fear	-1.376	90.000
Real Fear > Virt Anger	-2.352	167.000
Real Fear > Virt Disgust	0.075	78.000

Continued on next page

Table B.1: Group level t -tests and Sum of Significantly different channels averaged across ROIs.

Contrast	Mean t value	Sum of Sig. diff channels
Real Fear > Virt Sadness	1.073	118.000
Real Fear > Virt Neutral	0.983	101.000
Real Fear > Virt Surprise	1.805	136.000
Real Anger > Real Disgust	2.054	158.000
Real Anger > Real Sadness	0.545	113.000
Real Anger > Real Neutral	1.915	191.000
Real Anger > Real Surprise	1.773	115.000
Real Anger > Virt Joy	1.931	141.000
Real Anger > Virt Fear	-0.996	85.000
Real Anger > Virt Anger	-1.887	70.000
Real Anger > Virt Disgust	0.840	103.000
Real Anger > Virt Sadness	1.050	134.000
Real Anger > Virt Neutral	1.744	109.000
Real Anger > Virt Surprise	1.377	217.000
Real Disgust > Real Sadness	-1.856	106.000
Real Disgust > Real Neutral	0.347	124.000
Real Disgust > Real Surprise	-0.980	130.000
Real Disgust > Virt Joy	-0.600	96.000
Real Disgust > Virt Fear	-2.206	146.000
Real Disgust > Virt Anger	-2.606	284.000
Real Disgust > Virt Disgust	-1.452	66.000
Real Disgust > Virt Sadness	-0.670	121.000

Continued on next page

Table B.1: Group level t -tests and Sum of Significantly different channels averaged across ROIs.

Contrast	Mean t value	Sum of Sig. diff channels
Real Disgust > Virt Neutral	-0.843	83.000
Real Disgust > Virt Surprise	-0.139	69.000
Real Sadness > Real Neutral	1.797	128.000
Real Sadness > Real Surprise	1.771	97.000
Real Sadness > Virt Joy	1.686	124.000
Real Sadness > Virt Fear	-0.656	33.000
Real Sadness > Virt Anger	-2.204	80.000
Real Sadness > Virt Disgust	-0.303	56.000
Real Sadness > Virt Sadness	0.713	107.000
Real Sadness > Virt Neutral	1.475	47.000
Real Sadness > Virt Surprise	2.301	104.000
Real Neutral > Real Surprise	-0.638	173.000
Real Neutral > Virt Joy	-1.072	67.000
Real Neutral > Virt Fear	-2.179	255.000
Real Neutral > Virt Anger	-2.525	322.000
Real Neutral > Virt Disgust	-2.123	139.000
Real Neutral > Virt Sadness	-0.900	151.000
Real Neutral > Virt Neutral	-0.988	102.000
Real Neutral > Virt Surprise	0.344	143.000
Real Surprise > Virt Joy	0.824	120.000
Real Surprise > Virt Fear	-2.407	136.000
Real Surprise > Virt Anger	-2.482	167.000

Continued on next page

Table B.1: Group level t -tests and Sum of Significantly different channels averaged across ROIs.

Contrast	Mean t value	Sum of Sig. diff channels
Real Surprise > Virt Disgust	-1.044	80.000
Real Surprise > Virt Sadness	-0.182	73.000
Real Surprise > Virt Neutral	0.162	104.000
Real Surprise > Virt Surprise	0.883	88.000
Virt Joy > Virt Fear	-1.810	166.000
Virt Joy > Virt Anger	-2.421	189.000
Virt Joy > Virt Disgust	-1.524	129.000
Virt Joy > Virt Sadness	-0.185	118.000
Virt Joy > Virt Neutral	-0.695	103.000
Virt Joy > Virt Surprise	-0.287	80.000
Virt Fear > Virt Anger	-1.766	51.000
Virt Fear > Virt Disgust	1.338	72.000
Virt Fear > Virt Sadness	1.757	125.000
Virt Fear > Virt Neutral	2.267	114.000
Virt Fear > Virt Surprise	2.356	153.000
Virt Anger > Virt Disgust	2.054	138.000
Virt Anger > Virt Sadness	2.488	170.000
Virt Anger > Virt Neutral	2.373	128.000
Virt Anger > Virt Surprise	2.616	207.000
Virt Disgust > Virt Sadness	1.327	74.000
Virt Disgust > Virt Neutral	1.005	39.000
Virt Disgust > Virt Surprise	1.471	153.000

Continued on next page

Table B.1: Group level t -tests and Sum of Significantly different channels averaged across ROIs.

Contrast	Mean t value	Sum of Sig. diff channels
Virt Sadness > Virt Neutral	-0.015	100.000
Virt Sadness > Virt Surprise	1.176	82.000
Virt Neutral > Virt Surprise	0.943	99.000

Appendix C

Memory Task ANOVA Table

Table C.1: Two-way ANOVA results for the effect of Face Type and Emotion and their interaction on the correct responses.

	sum_sq	df	F	PR(>F)
Intercept	261.07756	1.00000	1764.58989	0.00000
C(Face_Type)	1.17722	1.00000	7.95666	0.00481
C(Emotion)	0.73335	6.00000	0.82610	0.54946
C(Face_Type):C(Emotion)	0.40872	6.00000	0.46041	0.83797
Residual	710.47356	4802.00000		